AR-009-445

DSTO-TR-0196

Orion P3C Horizontal Stabiliser Strain Survey and Corrosion Repair Development

R.H. Kaye, R. Jones and P. Hayes

DEPARTMENT ◆ OF DEFENCE

DEFENCE SCIENCE AND TECHNOLOGY ORGANISATION

DISCLAIMER NOTICE

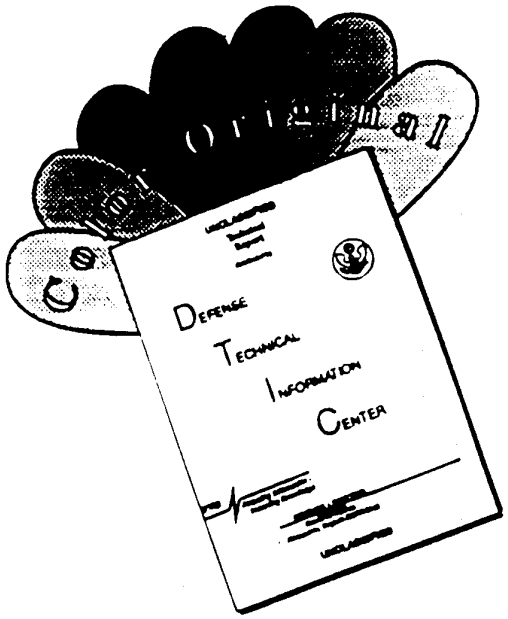

THIS DOCUMENT IS BEST QUALITY AVAILABLE. THE COPY FURNISHED TO DTIC CONTAINED A SIGNIFICANT NUMBER OF COLOR PAGES WHICH DO NOT REPRODUCE LEGIBLY ON BLACK AND WHITE MICROFICHE.

Orion P3C Horizontal Stabiliser Strain Survey and Corrosion Repair Development

R.H. Kaye, R. Jones and P. Hayes*

Airframes and Engines Division
Aeronautical and Maritime Research Laboratory

DSTO-TR-0196

ABSTRACT

This report presents results of an experimental investigation into the stress/strain field at the lower skin root region of the P3 horizontal stabiliser. Thermo elastic and strain gauge methods were used with a bare structure P3 tail-plane loaded under laboratory conditions. Applied load was restricted to 60% of design limit by the nature of the test article and the loading rig. The results show that the stresses in the region of interest are predominantly spanwise in direction. Stress concentrations consisting typically of 30% in-plane shear stress and 70% spanwise stress were found to occur near the inboard corners of each of the three lower skin planks. The largest of these was found at the forward corner of the forward plank. The load transfer between the skin panels and the spars was found to take place over the inboard 100mm of the stabiliser.

A bonded repair to corrosion damage has been presented on the basis of the bonded joints in the repair being stronger than the surrounding parent material. This repair design is not in any way dependent on the stress/strain test results and falls within the requirements of the recently produced RAAF Engineering Standard C5033. The region has a complex stress distribution due to the stabiliser skin panels terminating at the fuselage. Laboratory investigation of this stress distribution has been brought about by the availability of a suitable test article and has provided valuable ancillary information.

* Professor of Solid Mechanics, School of Mechanical Engineering
Monash University, Clayton, Victoria

RELEASE STATEMENT

Approved for public release

DEPARTMENT OF DEFENCE

DEFENCE SCIENCE AND TECHNOLOGY ORGANISATION

Published by

DSTO Aeronautical and Maritime Research Laboratory
PO Box 4331
Melbourne Victoria 3001

Telephone: (03) 626 8111
Fax: (03) 626 8999

AR No. 009-445
November 1995

APPROVED FOR PUBLIC RELEASE

Orion P3C Horizontal Stabiliser Strain Survey and Corrosion Repair Development

Executive Summary

The purpose of this report is to publish results of structural testing of an Orion P3 tail plane. This testing was performed partly in support of a proposed bonded repair to corrosion damage that has been found to occur in the stabiliser skin of fleet aircraft. This repair is more economical to install and more durable than the standard repair which uses many additional drilled holes for mechanical fasteners. This repair is presented with an explanation how it falls within the requirements of the relevant RAAF Engineering Standard.

Authors

R.H. Kaye
Airframes and Engines Division

Mr Robert Kaye joined DSTO at AMRL in 1990 as a structural engineer with a background in full scale structural testing. The first three years at AMRL were spent in evaluation of bonded repairs primarily using finite element methods. Included, was the analysis of repairs to fuselage skin lap-joints, wing skin planks and bulkhead frames. More recently he has been involved with structural and mechanical aspects of full scale fatigue test installations.

R. Jones

Professor Jones graduated in 1969 with a Bachelor of Science (first class honours) and received his Doctor of Philosophy in 1973 from Adelaide University. Prior to joining Monash University in 1993, Professor Jones was a Research Leader in the Airframes & Engines Division, DSTO, Aeronautical Research Laboratory. He is currently the Chairman, Department of Mechanical Engineering, Monash University. Professor Jones is very active in the areas of structural integrity assessment, structural repairs/reinforcement and computational mechanics.

P. Hayes
Airframes and Engines Division

After five years in the RAAF as an Aeronautical Engineer Mr Peter Hayes joined AMRL in 1989. Since then he has been partly involved with structural and mechanical design of aircraft component test rigs. To a greater extent Mr Hayes has taken a role in data acquisition design and procurement. Recently his work has been focussed on a complex multi-channel structural testing control and data acquisition system. He has also been involved with aircraft flight trials for the purposes of flight loads monitoring.

Contents

1. Introduction

In recent years P3 - Orion aircraft in service with the Royal Australian Air Force have experienced corrosion damage to skin panels at the root of the horizontal stabiliser. The lower root fairing attachment fastener holes are common corrosion sites, see Figure 1. The standard repair for this damage involves a series of mechanically fastened doublers and requires numerous additional fastener holes to be drilled through the skin panels [1]. The latter part of this report details an alternative repair which uses a bonded doubler and therefore requires minimal use of additional mechanical fasteners. This repair would do less irreversible damage to the structure and is expected to have a longer fatigue life due to the reduction of fastener hole stress concentrations.

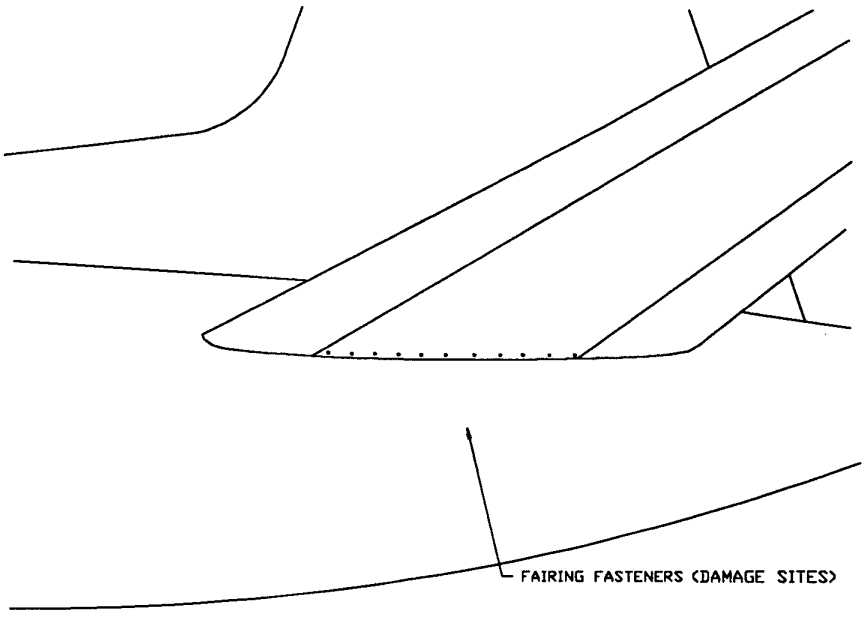

Figure 1: Corrosion Damage Locations

1.1 Structural Testing

The test article was the bare structure of a discarded P3 aft fuselage and tail plane. Measurement of the stress/strain distribution has been performed using thermo-elastic and strain gauge methods. Strains were found to be linear with load over the test range nil - 60% of limit.

1.2 Testing to Higher Loads

Static loading to the design ultimate condition could not be readily achieved due to the fuselage structure being incomplete and the large stabilator tip deflections that would result. Fuselage and test rig modifications would allow such a test to proceed however it is highly likely that both repairs would easily survive as the primary bending loads are carried by the spar caps at the root region.

1.3 Proposed Bonded Repair

Bonded doubler skin repairs have been extensively investigated in [2,3,4,5,6]. In this case, the damage sites are close to the connection with the fuselage skin and the normal overlap distances are not available. A more novel repair design using a skin panel cut-out and bonded doubler has been proposed [11] and is described in section 4. The standard repair and the bonded repair were installed on opposite sides of the test article and thermo-elastic data from the surrounds of the repair has been collected.

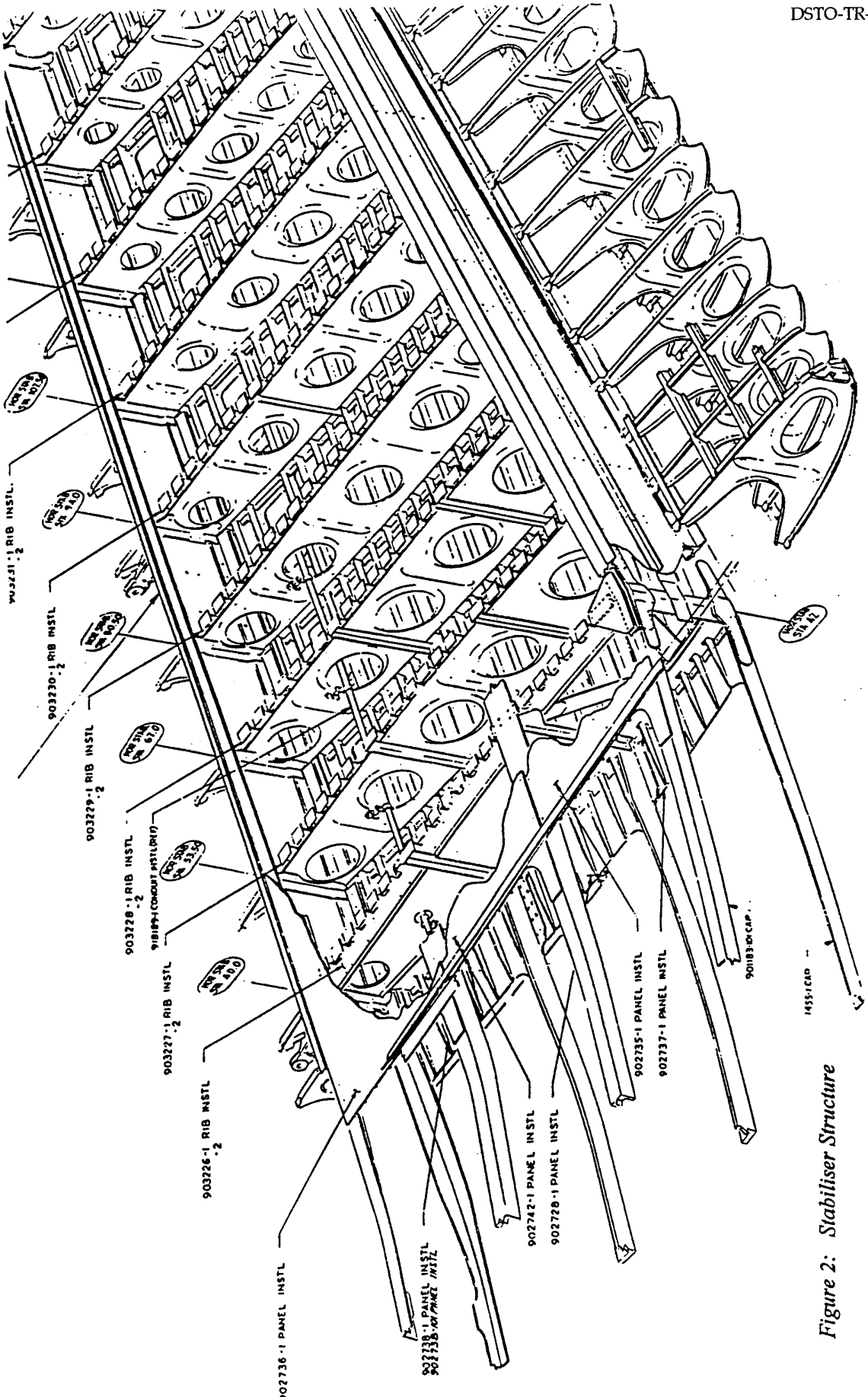

Figure 2: Stabiliser Structure

2. Thermo-Elastic Stress Survey

2.1 Description of Structure

The stabiliser skin near the root consists of three planks each having seven integral stiffeners running spanwise. The planks meet over two heavier T-section spar caps that continue through the fuselage as shown in Figure 2. Two fully webbed spars, also continuous through the fuselage, make up the main cell which provides most of the bending and torsional strength at the root region. The skin planks terminate at the fuselage skin, except for some support structure inboard of the forward plank (not shown in Figure 2). The spanwise loads in the skin planks are therefore expected to transfer to the four continuous members outboard of the fuselage connection.

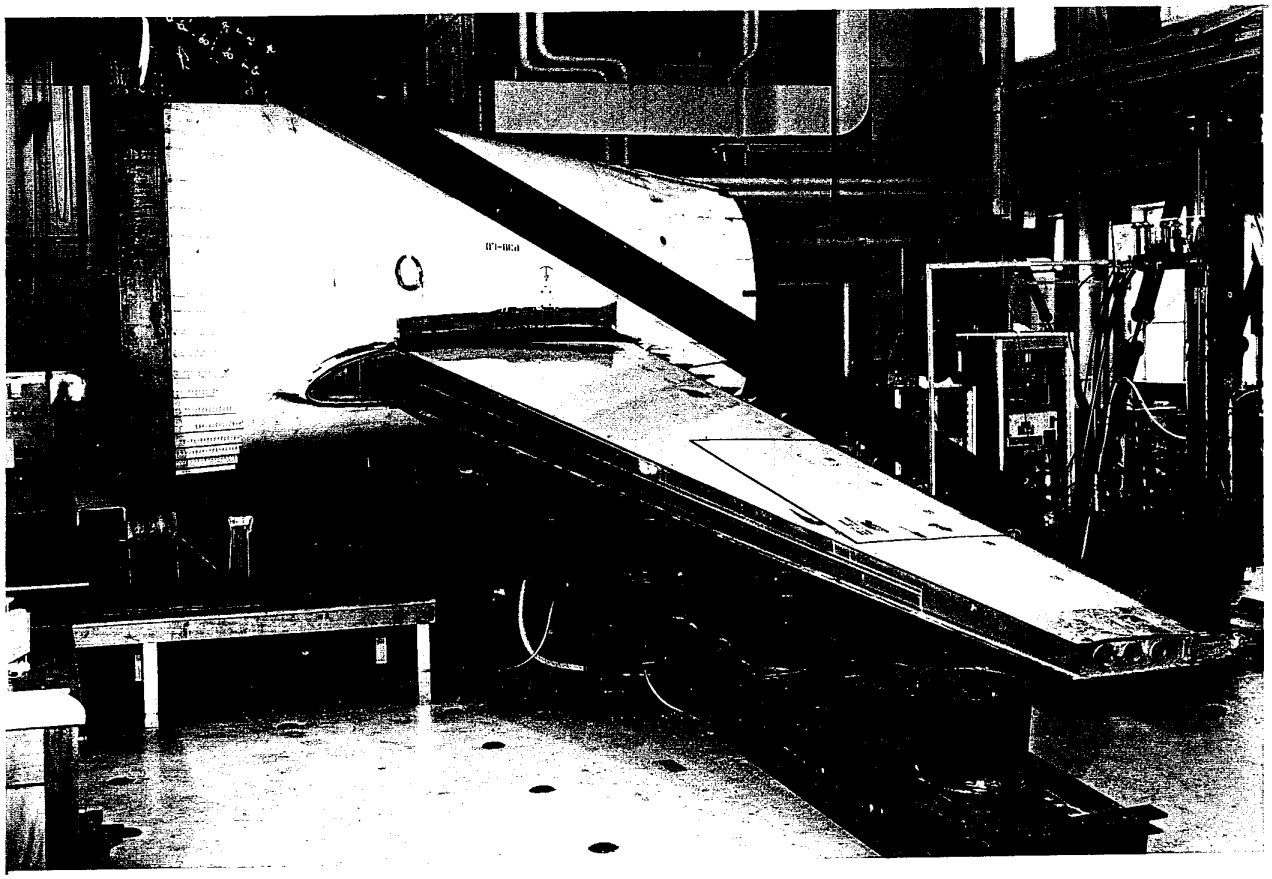

Figure 3: Test Article and Loading Rig

2.2 Description of Thermo-Elastic Scanning Procedure

With the vertical stabiliser removed, the empennage was inverted and mounted to the laboratory strong floor using a structural steel frame, (Figure 3). An experimental evaluation of the load transfer at the root region was then obtained using thermal emission techniques. This was performed using a commercially available infra-red camera, trade name "SPATE", (see Figure 4).

The relationship between the thermal emission of a body under cyclic loading and the local stress distribution is given in [7,8]. In each case the scanned regions, (see Figures 6 to 13), were sprayed matt black to achieve a uniformly high infra-red emissivity. These regions were also surrounded by masking tape which can be seen at the edges of each scan where the signal is very low. The stabiliser was loaded via a mechanical shaker consisting of an out-of-balance rotating mass, remote motor with speed controller, and a flexible drive cable. The rotating mass was fastened to the stabiliser tip at mid-chord and driven at a speed of approximately 420 rpm.

2.3 Magnitude of Stresses Being Scanned

In order to determine the general magnitude of the stress field being scanned a rosette strain gauge was located on the external skin surface between the second and third fairing fasteners. The resulting values were:

110 microstrain spanwise,

11 microstrain at 45 degrees

8 microstrain chordwise.

2.4 Discussion of Results

Despite the low signal levels, the SPATE results clearly show the load transfer from the skin planks to the continuous members. The plotted quantity is proportional to the bulk stress (sum of the principal stresses). The peak stresses are concentrated in small regions near the inboard corners of each plank as expected. Away from the spars at the root the stresses in the skin are very low except in the forward plank which has more restraint along its inboard edge. The load transfer region (transfer between the skin planks and the spar caps) is shown to be confined to the inboard 100mm of stabiliser.

It is interesting to note that, in Figure 9, the full depth internal rib frame can be seen as a region of lower signal. Close examination of the figures also reveals that the fasteners coupling the skin to the trailing edge spar can be seen as regions also with low infra-red signatures. The stress pattern at an open fastener hole in the stabiliser skin is shown in Figure 13. Here the orientation of the stress pattern around the hole reveals the direction of the principle stresses in the region.

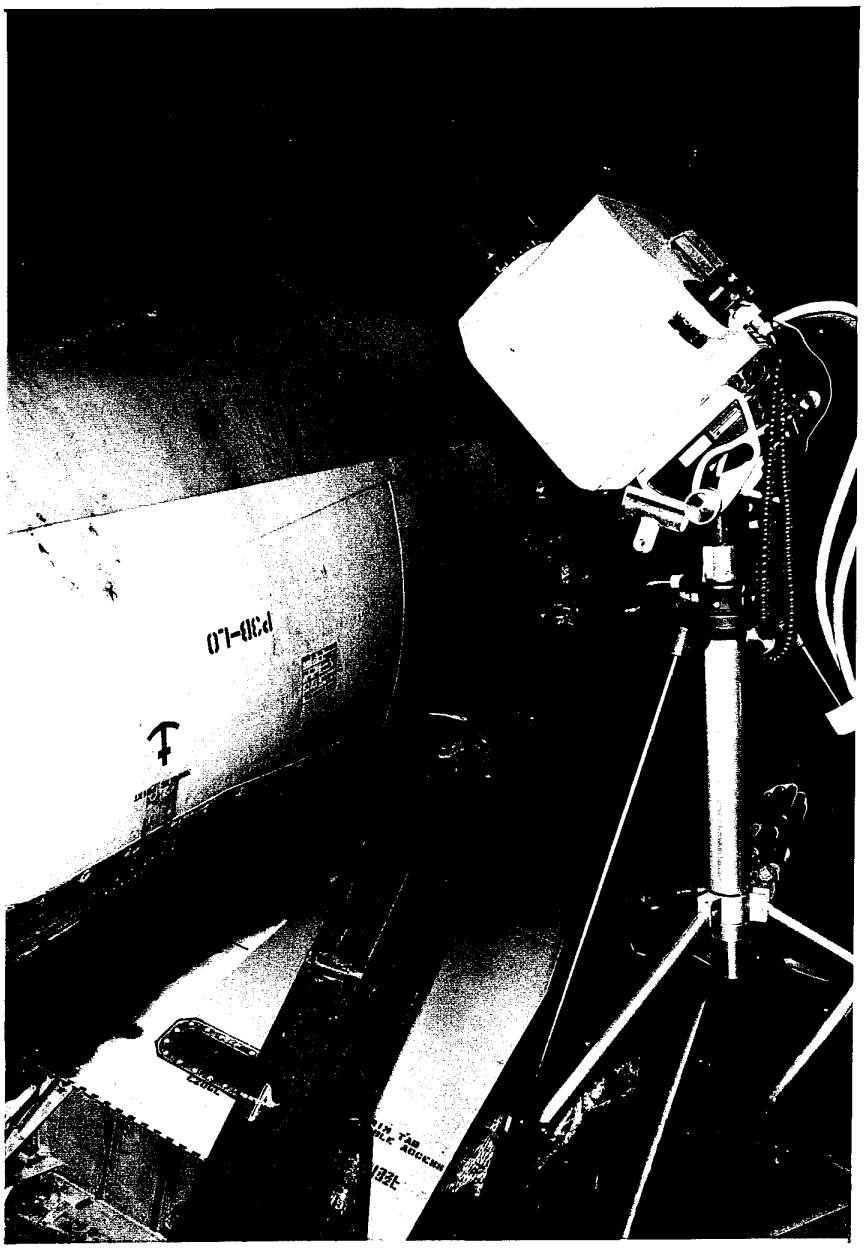

Figure 4: SPATE Camera Focussed on Stabilator Root

3. Strain Gauge Survey

3.1 Loading Arrangement

With the P3 empennage in the inverted position, loading was applied in an upwards direction to both horizontal stabilisers, ie. down-loading in the sense of the inverted tail plane. Ten air bags were used, operating at a common variable pressure and reacting against the laboratory strong floor. These were spaced spanwise (as per Figure 14) so as to produce, as near as possible, the bending moment distribution given in Figure 15. Figure 15 is a reproduction of the ultimate load negative-checked-pitching-manoeuvre bending moment distribution from [9]. All of the air-bags were positioned along the 33% spar line.

3.2 Loading Sequence

For the strain survey, load was applied up to 60% of limit load in six steps of 10%. Strain readings were taken at each step on loading and at the 40%, 20% and zero levels during unloading.

3.3 Processing of Results

Rosette strain gauges were fitted at 17 places on the lower skin root region and 9 single gauges were placed on the lower spar caps. Gauge locations are shown in Figures 16 and 17. The strain results (Table 1) have been plotted against load and all gauges were found to give linear results. All gauges returned to zero on unloading. The 60% load rosette values have been converted to spanwise, chordwise and shear stresses using the linear elastic formulae and assuming uniform stress through the thickness (Table 2). The Von Mises equivalent stress was also calculated and is given as a percentage of the material ultimate stress. As with any strain survey, no information is obtained regarding initial residual strains at zero load. These may be caused during manufacture or by previous loading cycles. Only the change in strain due to the applied load is measured and it is assumed that residual strains are small in comparison.

3.4 Spanwise Components of Stress

These stresses (shown at their locations in Figure 18) are the primary bending stresses brought about by the skin planks and spar caps acting as flanges of a box beam separated by the spar webs and rib frames. As they are measured on the lower surface with the bending being in a downwards direction all spanwise stresses are compressive.

Variations in the spar stresses are brought about by their proximity to the loading line and differences in section areas. Values are all low enough to suggest that the stabiliser root would easily survive ultimate design load.

High skin stresses in the forward corner of the forward plank (also revealed in the SPATE plots) suggest that the skin provides the stiffer path into the fuselage carrry-through structure than the forward spar cap. The skin has about double the spanwise strain of the spar cap. The values suggest that yielding would only occur above design limit load. In that case, some of the load would be shed into the forward spar cap.

The value of 65 Mpa in the middle of the forward plank and the value of only 17 Mpa near the middle of the centre plank is a good guide to the differences in spanwise edge restraint which were also observed in the thermo-elastic images.

3.5 Shear Components of Stress

The sign and magnitude of the shear stress values (Figure 19) show the effect of the load transfer into the spar caps. The change in sign from one side of the spar caps to the other is strong evidence of this load transfer. Away from the root region the very low values show that stabiliser torsion has a minimal effect on skin shear stress. A separate strain survey was performed using a 25% spar line for loading instead of a 33% spar line. The net change in shear stress was quite uniform across all the gauges and for the outboard gauges, only about +6 MPa (Table 3).

4. Proposed Bonded Repair

4.1 Repair Configuration

The damage sites are typically centred within 45 mm from the edge of the skate angle at the fuselage skin connection. There is not sufficient overlap distance inboard of the damage to transfer the load from a normal bonded doubler back into the skin. This repair option, from [11], is based on the removal of a rectangular section containing the corrosion damage and is shown below in Figure 5. This rectangle extends underneath the skate angle to the end of the skin panel. The removed skin is replaced and stiffened against buckling and bending with a length of channel section and spacer on the inside. A bonded doubler of the same material is applied to the outside to transfer the load from the outboard skin to the insert. The insert picks up the fasteners in the skate angle in the same way as the original material but with a reinforcing strap underneath which picks up two extra fasteners. This repair has the advantage that it can cope with full thickness damage, up to and underneath the skate angle.

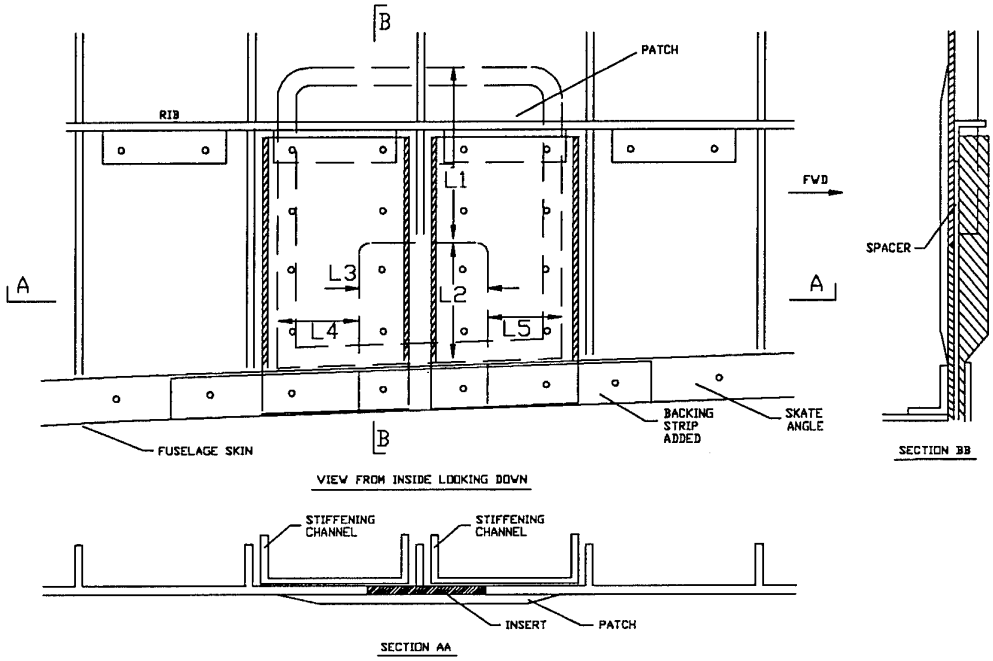

Figure 5: Proposed Bonded Repair

4.2 Integrity of the Bonded Repair

The procedures for designing a supported, single overlap bonded repair such as the one studied in this report are detailed in the RAAF Engineering Standard C5033 [13]. The standard has been refined over many years and, at the time of writing, is very close to being released. The repair studied in this report is based on a design [11] which was analysed in 1991 using an earlier version of [13]. It was therefore decided to re-run the analysis using the latest version of [13]. The analysis is provided in the appendix for a repair at FS 1188 where the skin thickness is 2.1mm. The only notable change from earlier work in [11] is an increase in the required overlap distance. This is caused by the use of a lower value of the adhesive shear modulus and a doubling in length of the required elastic trough.

The analysis used applies to a symmetric double lap joint in a unidirectional stress field. In the application of the analysis to the specific repair region and arrangement the following assumptions have been made:

a) That the skin in the region is stiffened against out-of-plane bending such that the single sided lap joints in the repair can be treated as one side of a double lap joint.

b) That the chordwise direction is essentially un-loaded and that chordwise strains are less than those caused by spanwise load Poisson Ratio effects.

c) That the mixture of shear and spanwise stress is a less severe loading case for the repair than a purely unidirectional stress field.

The results of the analysis show that the design is feasible. A repair which incorporates the characteristics detailed and calculated in this analysis can be expected to be a satisfactory, airworthy repair. The analysis shown here cannot however be considered to be a complete repair design package. A repair analysis which applies these same checks to the individual repair case being examined must be produced and checked. This would then form a key element of the complete repair design package. Other essential elements of the repair package would include details of the surface preparation and repair application procedures to be used. The details provided in [13] are an invaluable aid in specifying these items.

4.3 Stress Field Outside of the Repair

Figure 22 and 23 are SPATE scans of both repairs plus the surrounding regions. Both repairs show a small increase in stress immediately outboard of the edge of the repair. This is caused by the increase in stiffness that occurs locally with both repair types. For a bonded doubler on a flat plate of equivalent stiffness to the plate, and a subjected to a unidirectional stress field, this stress increase is at worst 12%. The stresses in this region that have been presented in earlier sections are low enough to cope easily with this increase. Stress concentrations around fastener holes do not show up in these Figures due to the size of the region being scanned and the resolution of the SPATE system. For similar reasons the stresses around the bonded repair in Figure 23 are appear more pronounced.

5. Conclusion

Stress/strain survey of the full scale P3C test article by thermo-elastic and strain gauge methods have found that stresses are low at all the potential damage sites except the forward most site on each side of the aircraft. Stress concentrations comprising of about 30% shear and 70% spanwise have been found at the inboard corners of each of the three planks. The stress concentration at the forward corner of the forward plank is more severe and is likely to cause localised yielding in the skin at loads beyond design limit load. A uniform spanwise stress was found to exist across the forward plank on each side of the aircraft in addition to the concentrations at the skin plank corners.

The proposed bonded repair presented above has been shown analytically to have bond strengths greater than material ultimate strength. This analysis is known to be conservative with respect to experimental results. The proposed repair has also been shown to fall within the design requirements of the RAAF Engineering Standard [13] and does not require further testing or analysis. The experimental work that has been reported here is the result of a suitable test article being available rather than a pre-requisite to validation of the repair design but has provided detailed knowledge of the repair region that is not normally available.

6. Acknowledgments

The authors wish to acknowledge the following people whose work has been reported in this document.

Mr. R. Bailey, Mr. B. Dingley and Mr N Manger for their work in preparing the full scale test rig structural and mechanical systems.

Mr. D. Rowlands for his work in conducting the thermal emission surveys of the full scale test article.

Mr P. Ferrarotto, Mr N. Hall and Mr M. Borg for their work in preparing the strain survey of the full scale test article.

FltSgt T Barton (RAAF) and Cpl T. Thomson (RAAF) for their work in installation of the repairs to the test article.

Mr M. Davis for his work on the initial concept and design of the bonded repair.

Mr K. Walker for provision of the updated repair calculations presented in the appendix.

FltLt M. Graham (RAAF) and SqnLdr A. Dale (RAAF) as the initial task sponsors for their work in providing the full scale test article, P3 design documentation and general RAAF liaison.

References

1. NAVAIR, P3 Structural Repair Manual, NAVAIR 01-75PAA-3-1.

2. L. Molent, N. Bridgford, D. Rees and R. Jones, Environmental Evaluation of Repairs to Fuselage Lap Joints, Composite Structures, 21,121-130,1992.

3. L. Molent, R. J. Callinan and R. Jones, Structural Aspects of the Design of an all Boron Epoxy Reinforcement for the F111C Wing Pivot Fitting: Final Report, ARL, Aircraft Structures Report 436, September 1992.

4. R. Jones, N. Bridgford, L. Molent and G. Wallace, Bonded Repair of Multi-Site Damage, pp 199-213, Structural Integrity of Aging Airplanes, edited by S. N. Atluri, S. G. Sampath and P. Tong, Springer Verlag, Berlin/Hieldelberg, 1991.

5. U. G. Goranson and M. Miller, Aging Jet Structural Evaluation Programs. Presented at 15th ICAF Symposium, Jerusalem, Isreal, June 21-23,1989.

6. A. A. Baker and R. Jones, Bonded Repair of Aircraft Structures, Martinus Nijhoff, The Netherlands, 1988.

7. A. K. Wong, R. Jones and J. G. Sparrow, Thermoelastic Constant or Thermoelastic Parameter, J. Phys. Chem. of Solids, 48, pp 749-753, 1988.

8. W. Thomson (Lord Kelvin), On the Thermo-Elastic and Thermo-Magnetic Properties of Matter, Q. J. Maths, 1, 55-77, 1855, reprinted in Phil. Mag., 5, 1878.

9. F. M. Hoblit, D. L. Bakalar and H. I. MacDonald, Structural Design Loads - P3V - 1 Part III - Empennage, Lockheed Aircraft Corporation, LR 13167 - III, December 1960.

10. L. J. Hart-Smith, Adhesively Bonded Double Lap Joints, NASA Langley Research Center Report NASA CR-112235, January 1973.

11. M. J. Davis, P3 Corrosion Repair, Minute to R. Jones, ARL dated 19/4/91.

12. Aerospace Structural Metals Handbook, Aeronautical Systems Division, Wright Patterson Airforce Base, March 1963.

13. RAAF Engineering Standard C5033 - Composite Materials and Adhesive Bonded Repairs, Headquaters Logistics Command RAAF, 1995.

Appendix

Repair Calculations

ADHESIVE PROPERTIES

FM73 FILM ADHESIVE (60 deg C CONDITIONS)

ADHESIVE THICKNESS		ADHESIVE SHEAR MODULUS		ADHESIVE SHEAR STRESS	
$\eta := 0.13$	mm	$G := 248$	MPa	$\tau_p := 18.1$	MPa

YOUNG'S MODULUS

$\mu := 0.33$ $\quad E_c := 2 \cdot G \cdot (1 + \mu)$ $\quad E_c = 659.68$ MPa

ADHESIVE STRAINS ELASTIC $\gamma_e := 0.073$ PLASTIC $\gamma_p := 1.357$

CURE TEMPERATURE $T_{cure} := 120$ deg C

PARENT MATERIAL PROPERTIES

SKIN THICKNESS	$t_i := 2.1$	mm	$t_{min} := 2.1$	mm
YIELD STRESS	$\sigma_{yi} := 460$	MPa		
ULTIMATE STRESS	$\sigma_{ui} := 517$	MPa		
FRACTURE TOUGHNESS	$K_c := 2600$	$Mpa \cdot \sqrt{mm}$		
YOUNGS MODULUS	$E_i := 69000$	MPa		
POISSON'S RATIO	$\nu := 0.3$			
THERMAL EXPANSION COEFFICIENT	$\alpha_i := 22.7 \cdot 10^{-6}$	(mm/mm)/C		
TEMP AT MAX LOAD	$T_{min} := 60$	deg C		

REPAIR PATCH MATERIAL

SAME AS PARENT MATERIAL

YOUNGS MODULUS	$E_o := 69000$	MPa
THERMAL EXPANSION COEFFICIENT	$\alpha_o := 22.7 \cdot 10^{-6}$	(mm/mm)/C

CALCULATE THE REQUIRED PATCH THICKNESS

$$t_o := \left(\frac{E_i}{E_o}\right) \cdot t_i$$

$t_o = 2.1$ mm

EVALUATE THE REPAIRABILITY BASED ON THE LOAD CAPACITY OF THE ADHESIVE

Calculate the potential load capacity of a single overlap joint, allowing for thermal stresses:

$\Delta T := T_{min} - T_{cure}$ $\Delta T = -60$ deg C

Load capacity is the lesser of P1 and P2:

$$\Phi := \left[2 \cdot \eta \cdot \tau_p \cdot \left(0.5\gamma_e + \gamma_p\right) \cdot E_i \cdot t_i \cdot \left(1 + \frac{E_i}{E_o} \cdot \frac{t_i}{t_o}\right)\right]^{0.5}$$

$P1 := \left(\alpha_o - \alpha_i\right) \cdot \Delta T \cdot 2 \cdot E_i \cdot t_i + \Phi$ $P1 = 1.37910^3$ N per mm

$$\phi := \left[2 \cdot \eta \cdot \tau_p \cdot \left(0.5\gamma_e + \gamma_p\right) \cdot E_o \cdot t_o \cdot \left(1 + \frac{E_o}{E_i} \cdot \frac{t_o}{t_i}\right)\right]^{0.5}$$

$P2 := \left(\alpha_i - \alpha_o\right) \cdot \Delta T \cdot 2 \cdot E_o \cdot t_o + \phi$ $P2 = 1.37910^3$ N per mm

THEREFORE $P := P2$ (or P1) $P = 1.37910^3$ N per mm

CHECK RAPID REPAIRABILITY CRITERION

$P_{RRC} := 1.2\sigma_{ui} \cdot t_i$ $P_{RRC} = 1.30310^3$

$MOS := \frac{P}{P_{RRC}} - 1$ MOS=0.058 Acceptable

CHECK THE STRUCTURAL INTEGRITY AND FATIGUE SUSCEPTIBILITY

Calculate the stress under the repair

$$N_{star} := \sigma_{ui} \cdot t_{min}$$

$$N_{star} = 1.086 \cdot 10^{3} \quad \text{N per mm}$$

However in this case the load intensity is known from the aircraft design calculations [9]. This value is conservative with respect to the measured data presented in Section 3:

$$N_{star} := 680 \quad \text{N per mm}$$

$$\sigma_{star} := \frac{N_{star}}{t_i}$$

$$\sigma_{star} = 323.81 \quad \text{MPa}$$

$$\Omega_L := 1.2$$

$$\Omega_T := 1.5$$

$$\sigma_o := E_i \cdot t_i \cdot \frac{\left[\Omega_L \cdot \sigma_{star} + \Omega_T \cdot E_i \cdot (\alpha_o - \alpha_i) \cdot \Delta T\right]}{(E_o \cdot t_o + E_i \cdot t_i)}$$

$$\sigma_o = 194.286 \quad \text{MPa}$$

Check the adhesive shear strain

$$\lambda := \sqrt{\left(\frac{G}{\eta}\right) \cdot \left[\left(\frac{1}{E_i \cdot t_i}\right) + \left(\frac{1}{E_o \cdot t_o}\right)\right]} \qquad \lambda = 0.162$$

$$\gamma_{max} := \sigma_o \cdot t_i \cdot \frac{\lambda}{G} \qquad \gamma_{max} = 0.267$$

This value exceeds the elastic limit. The maximum strain is therefore given by:

$$\gamma_{max} := \left(\frac{\tau_p}{2 \cdot G}\right) \cdot \left[1 + \left(\sigma_o \cdot t_i \cdot \frac{\lambda}{\tau_p}\right)^2\right]$$

$$\gamma_{max} = 0.525$$

$$\gamma_{allow} := 0.8 \cdot (\gamma_e + \gamma_p)$$

$$\gamma_{allow} = 1.144$$

$$MOS := \left(\frac{\gamma_{allow}}{\gamma_{max}}\right) - 1 \qquad MOS = 1.18 \qquad \text{Acceptable}$$

Calculate the repaired stress intensity

$$K_{inf} := \sqrt{\frac{E_i \cdot \eta}{G} \cdot \left[\sigma_o \cdot \tau_p \cdot \left[1 + \left(\frac{\sigma_o \cdot \lambda \cdot t_i}{\tau_p} \right)^2 \right] - \frac{\tau_p}{\lambda \cdot t_i} \cdot \left[1 + 2 \cdot \left(\frac{\sigma_o \cdot \lambda \cdot t_i}{\tau_p} \right)^3 \right] \right]}$$

$K_{inf} = 1.28 \cdot 10^3$ MPa$\cdot\sqrt{mm}$

$K_{allow} := 0.8 K_c$ $K_{allow} = 2.08 \cdot 10^3$ MPa$\cdot\sqrt{mm}$

$MOS := \frac{K_{allow}}{K_{inf}} - 1$ $MOS = 0.625$ Acceptable

Check the structural integrity of the patch

$$\sigma_p := E_o \cdot t_o \cdot \frac{\Omega_L \cdot \sigma_{star} + \Omega_T \cdot E_i \cdot (\alpha_o - \alpha_i) \cdot \Delta T}{(E_o \cdot t_o + E_i \cdot t_i)}$$

$\sigma_p = 194.286$ MPa

$\varepsilon_p := \frac{\sigma_p}{E_o}$ $\varepsilon_p = 0.003$

$\sigma_{uo} := \sigma_{ui}$

$\sigma_{allow} := \sigma_{uo}$

$MOS := \frac{\sigma_{allow}}{\sigma_p} - 1$ $MOS = 1.661$ Acceptable

Calculate peel stresses

$$E_{cprime} := \frac{1}{\left(\frac{1}{E_c} + \frac{2}{E_i} + \frac{4}{E_o} \right)}$$ $E_{cprime} = 623.891$ MPa

$$\sigma_{cmax} := \tau_p \cdot \left[\frac{3 \cdot E_{cprime} \cdot t_o \cdot (1 - \nu^2)}{E_o \cdot \eta} \right]^{0.25}$$ $\sigma_{cmax} = 14.383$ MPa

$\sigma_{callow} := 69$ MPa For toughened adhesive

$MOS := \frac{\sigma_{callow}}{\sigma_{cmax}} - 1.0$ $MOS = 3.797$ Acceptable

Check fatigue stress

$\sigma_f := 0.4 \sigma_{star}$ $\sigma_f = 129.524$ MPa

Calculate the stress under the patch

$$\sigma_{hash} := \frac{E_i \cdot t_i \cdot \left[\Omega_L \cdot \sigma_f + \Omega_T \cdot E_i \cdot (\alpha_o - \alpha_i) \cdot \Delta T\right]}{(E_o \cdot t_o + E_i \cdot t_i)} \qquad \sigma_{hash} = 77.714 \quad MP$$

Calculate shear strain in the adhesive at the fatigue stress

$$\gamma_{max} := \sigma_{hash} \cdot t_i \cdot \frac{\lambda}{G} \qquad \gamma_{max} = 0.107$$

This value exceeds the elastic limit. The maximum strain is therefore given by:

$$\gamma_{max} := \left(\frac{\tau_p}{2 \cdot G}\right) \cdot \left[1 + \left(\sigma_{hash} \cdot t_i \cdot \frac{\lambda}{\tau_p}\right)^2\right] \qquad \gamma_{max} = 0.107$$

$$\gamma_{allow} := 2 \cdot \gamma_e \qquad \gamma_{allow} = 0.146$$

$$MOS := \left(\frac{\gamma_{allow}}{\gamma_{max}}\right) - 1 \qquad MOS = 0.274 \quad \text{Acceptable}$$

DETERMINE THE PATCH DIMENSIONS

Primary Load Direction (Spanwise)

$$l_p := \frac{\sigma_{ui} \cdot t_i}{2 \cdot \tau_p} \qquad l_p = 30 \quad mm$$

$$l_e := \frac{3}{\lambda} \qquad l_e = 18.5 \quad mm$$

$$L_T := l_e + l_p \qquad L_T = 48.5 \quad mm \quad \text{Load Transfer Length}$$

$$L := 2 \cdot L_T \qquad L = 97 \quad mm \quad \text{Overlap Length}$$

97 mm is therefore a minimum value for L1 and L2 in Figure 5

Unloaded Direction (Chordwise)

$$l_p := \frac{\nu \cdot \sigma_{ui} \cdot t_i}{2 \cdot \tau_p} \qquad l_p = 9 \quad mm$$

$$l_e := \frac{3}{\lambda} \qquad l_e = 18.5 \quad mm$$

$$L_T := l_e + l_p \qquad L_T = 27.5 \quad mm \quad \text{Load Transfer Length}$$

$$L := 2 \cdot L_T \qquad L = 55 \quad mm \quad \text{Overlap Length}$$

55 mm is therefore a minimum value for L3, L4 and L5 in Figure 5

Table 1: Strain Survey Results for 60% of Limit Down Load Applied at Line of 33% Chord

Notes: Deflections in mm, strains in microstrain.
Negative strains are compressive.
LVDTs at port HS tip, fuselage and stbd HS tip.
Strain gauge locations are shown in Figures 16 and 17.
Test Date 10/12/92.

% LOAD	0	10	20	30	40	50	60	40	20	0
LVDTp	0	36	74	113	150	191	235	160	82	2
LVDTc	0	1	2	3	5	6	9	6	3	0
LVDTs	0	34	70	106	142	181	221	149	76	2
19	-1	-244	-491	-748	-982	-1245	-1509	-1009	-502	2
21	0	-246	-483	-721	-934	-1177	-1423	-928	-450	7
29	0	-226	-461	-708	-935	-1191	-1460	-991	-507	-16
23	0	-331	-670	-1017	-1332	-1683	-2025	-1376	-692	-1
25	-1	-272	-552	-845	-1113	-1412	-1717	-1172	-598	-12
27	0	-153	-312	-476	-626	-792	-961	-639	-318	-6
31	-1	-262	-509	-769	-1021	-1303	-1588	-1107	-563	22
33	0	-175	-356	-547	-719	-915	-1113	-735	-358	0
35	0	-168	-341	-517	-675	-853	-1030	-687	-338	1
1A	-1	-127	-254	-379	-488	-609	-735	-483	-237	1
1B	-1	-219	-441	-668	-873	-1106	-1347	-883	-431	2
1C	-1	-1	-6	-14	-23	-34	-52	-21	-10	-4
2A	0	-219	-431	-649	-846	-1061	-1273	-871	-445	-4
2B	0	59	134	219	305	403	516	332	156	6
2C	-1	16	35	58	86	118	158	127	77	8
3A	0	-33	-68	-103	-137	-175	-214	-140	-69	-2
3B	0	117	234	353	459	579	702	471	234	-4
3C	-1	-9	-15	-20	-24	-28	-31	-16	-7	0
4A	0	-143	-275	-405	-518	-642	-756	-523	-270	0
4B	-1	-15	-31	-46	-59	-73	-83	-43	-12	2
4C	0	-48	-89	-126	-153	-182	-199	-141	-70	4
5A	0	-167	-324	-482	-620	-770	-899	-595	-293	16
5B	0	-138	-281	-432	-575	-737	-903	-589	-281	4
5C	-1	8	18	27	36	50	59	24	2	-5
6A	0	-174	-339	-504	-648	-807	-944	-632	-316	11
6B	0	-130	-270	-417	-554	-709	-869	-581	-284	-2
6C	-1	23	47	72	94	122	144	79	31	-7
7A	-3	-157	-300	-443	-569	-705	-838	-584	-309	-5
7B	-1	-19	-32	-46	-55	-59	-49	-43	-25	1
7C	0	4	5	5	4	4	8	22	23	4
8A	0	-194	-382	-575	-747	-938	-1126	-763	-388	-4
8B	0	-19	-31	-43	-52	-64	-75	-55	-34	-3
8C	-1	29	59	90	119	148	179	139	80	6
9A	-1	-253	-500	-753	-982	-1235	-1490	-1030	-533	-7
9B	0	71	162	255	342	441	555	367	177	2
9C	0	66	139	221	304	403	526	361	191	1

Table 1 Continued:

% LOAD	0	10	20	30	40	50	60	40	20	0
10A	0	-186	-366	-547	-707	-885	-1055	-714	-361	-1
10B	0	-61	-124	-189	-249	-317	-385	-257	-128	0
10C	-1	33	62	88	109	132	150	106	56	-2
11A	0	-378	-778	-1202	-1596	-2044	-2525	-1701	-861	-11
11B	-1	12	35	60	77	85	77	75	28	-10
11C	0	82	182	286	387	497	623	468	269	5
12A	-1	-218	-436	-659	-862	-1088	-1312	-882	-443	-5
12B	0	-62	-126	-192	-252	-320	-388	-260	-130	-2
12C	0	71	143	217	286	363	438	294	146	0
13A	0	-208	-409	-613	-798	-1003	-1206	-821	-420	-3
13B	0	-17	-30	-44	-57	-71	-84	-64	-39	-3
13C	0	36	73	110	142	176	206	162	92	4
14A	-1	-118	-225	-331	-421	-518	-604	-424	-222	-1
14B	0	9	22	37	55	75	102	65	33	2
14C	0	-37	-76	-115	-149	-188	-226	-136	-60	0
15A	0	-198	-390	-585	-761	-953	-1143	-774	-393	2
15B	0	-75	-152	-235	-312	-399	-488	-325	-162	-2
15C	0	40	77	111	139	170	195	138	73	-3
17A	0	-231	-463	-703	-922	-1165	-1413	-957	-485	-5
17B	0	-86	-173	-266	-352	-450	-552	-369	-185	-5
17C	-1	71	144	219	289	366	444	301	152	-1
37A	-1	-122	-232	-341	-436	-537	-629	-444	-236	-2
37B	-1	15	33	52	70	95	131	88	47	1
37C	-1	-38	-76	-113	-146	-182	-217	-131	-56	4

Table 2: Skin Stresses for 60% of Limit Load (derived from Table 1)

Notes: Strains are in microstrain, stresses are in Mpa.
Negative values are compressive.
Rosette locations are shown in Figures 16 and 17.
Ultimate stress is for 7075-T6 material taken from [10].

Rosette Number	Spanwise Strain	Oblique Strain	Chordwise Strain	Spanwise Stress	Chordwise Stress	Shear Stress	Von Mises Stress	Percent of Ultimate Stress
1	-735	-1347	-52	-59	-21	52	104	21
2	-1273	516	158	-96	-17	-59	135	27
3	-214	702	-31	-17	-7	-45	79	16
4	-756	-83	-199	-64	-33	-22	67	13
5	-899	-903	59	-69	-16	26	77	16
6	-944	-869	144	-70	-11	26	79	16
7	-838	-49	8	-65	-19	-20	68	14
8	-1126	-75	179	-84	-12	-22	87	18
9	-1490	555	526	-104	6	-57	145	29
10	-1055	-385	150	-79	-13	-4	73	15
11	-2525	77	623	-182	-10	-56	202	41
12	-1312	-388	438	-92	3	-3	94	19
13	-1206	-84	206	-89	-12	-23	93	19
14	-604	102	-226	-52	-32	-28	67	13
15	-1143	-488	195	-85	-12	1	79	16
17	-1413	-522	444	-100	2	2	101	20
37	-629	131	-217	-54	-32	-30	70	14

Table 3: Skin Stresses for 60% of Limit Load Applied at Line of 25% Chord

Notes: Strains are in microstrain, stresses are in Mpa.
Rosette locations are shown in Figure 16 and 17.
Delta Shear Stress is the difference in shear stress due to the change in load line.

Rosette Number	Spanwise Strain	Oblique Strain	Chordwise Strain	Spanwise Stress	Chordwise Stress	Shear Stress	Delta Shear Stress
1	-714	-1387	-42	-57	-20	55	+3
2	-1254	418	147	-94	-18	-53	+6
3	-199	640	-23	-16	-6	-41	+3
4	-737	-241	-59	-59	-22	-9	+13
5	-890	83	-942	-94	-91	55	+29
6	-922	-896	164	-68	-9	28	+2
7	-832	-153	32	-64	-17	-13	+7
8	-1104	-141	187	-82	-11	-17	+5
9	-1484	422	516	-104	6	-49	+8
10	-1043	-436	162	-78	-12	0	+4
11	-2517	-33	620	-182	-11	-50	+6
12	-1313	-462	439	-92	4	1	+4
13	-1204	-179	219	-89	-11	-17	+5
14	-623	34	-179	-53	-29	-24	+4
15	-1142	-586	207	-84	-11	6	+5
17	-1422	-690	440	-101	1	11	+9
37	-677	38	-149	-56	-27	-25	+5

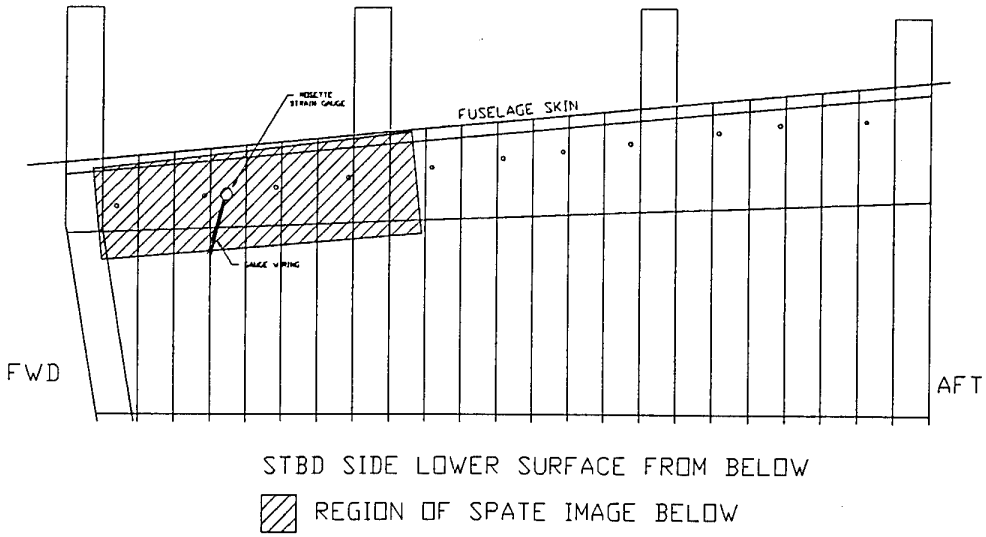

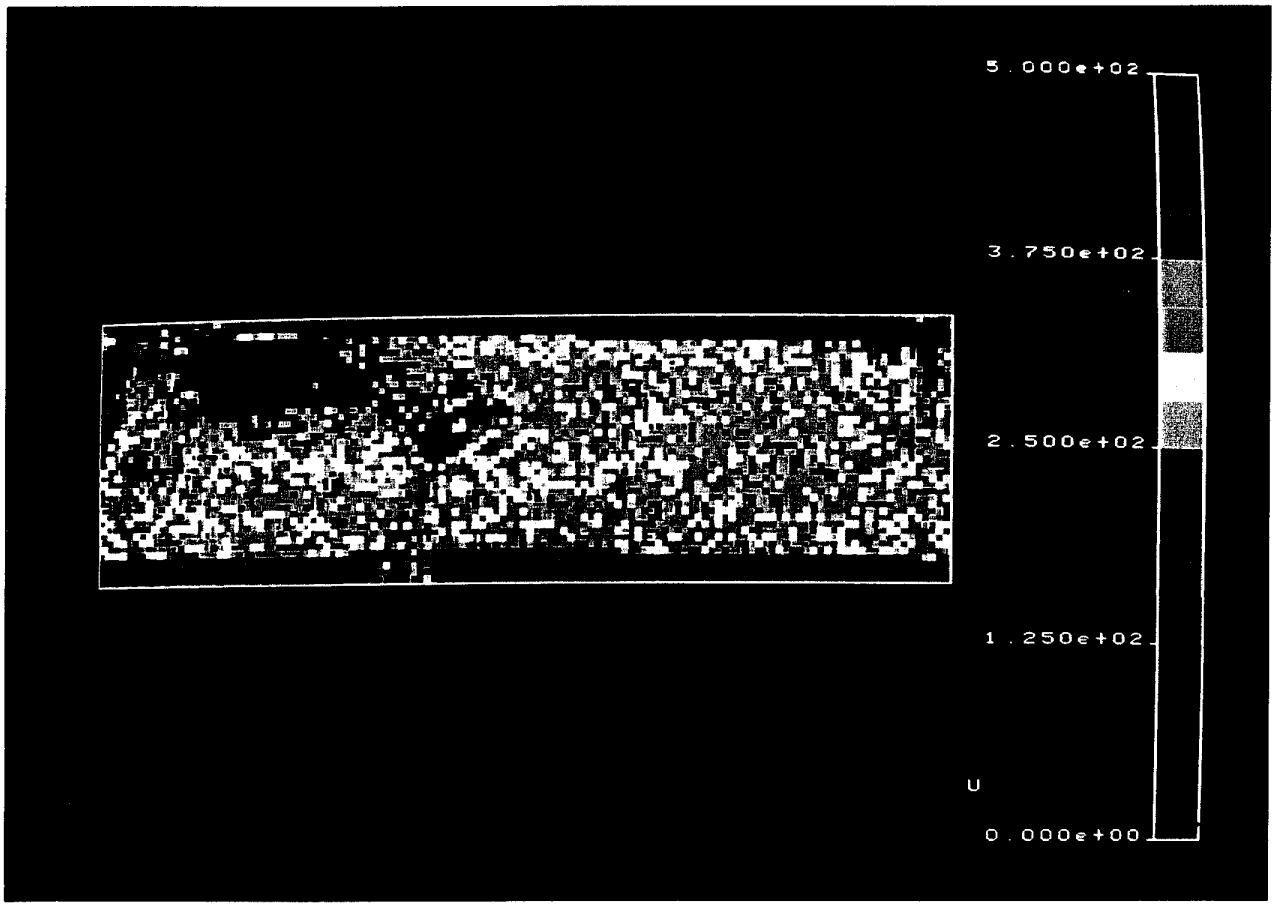

Figure 6: SPATE Region 1

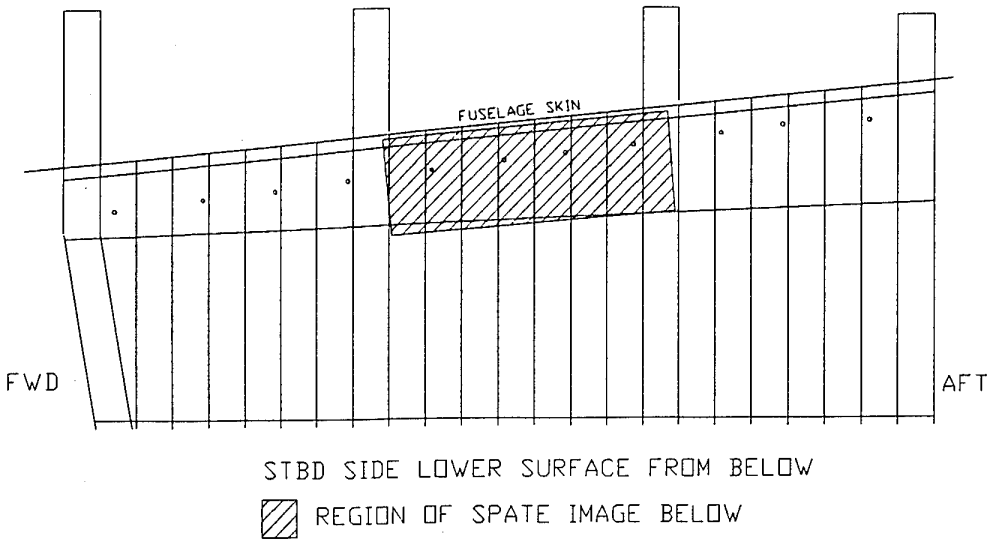

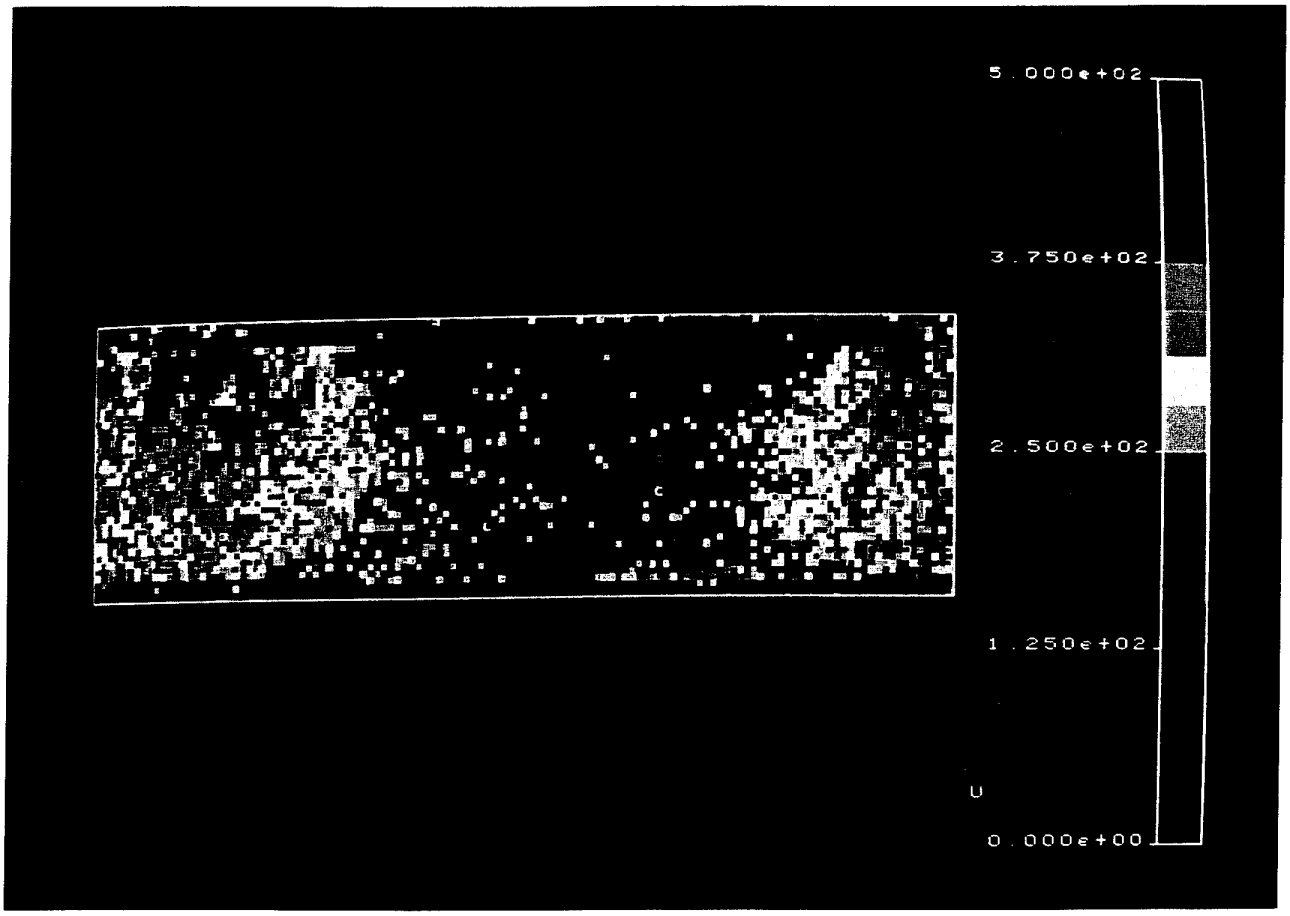

Figure 7: SPATE Region 2

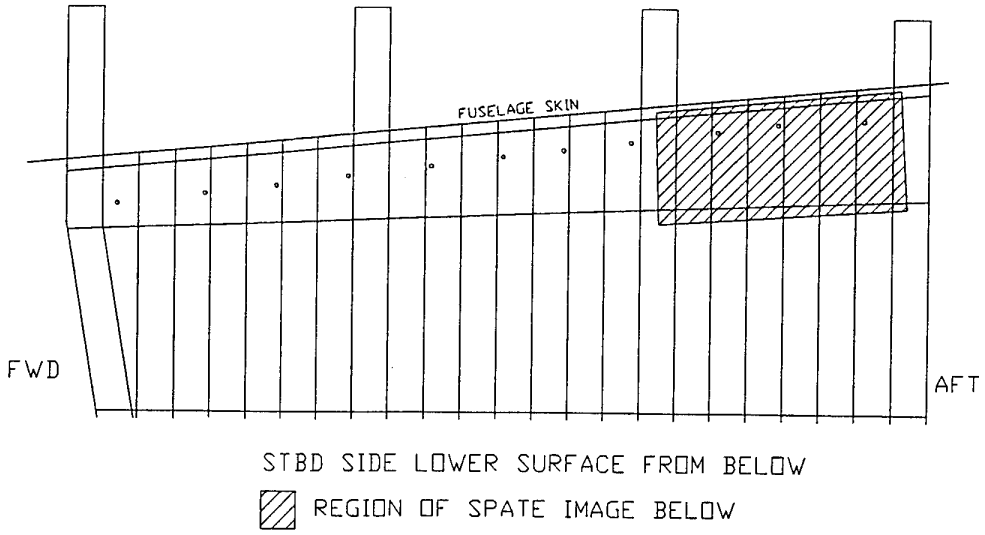

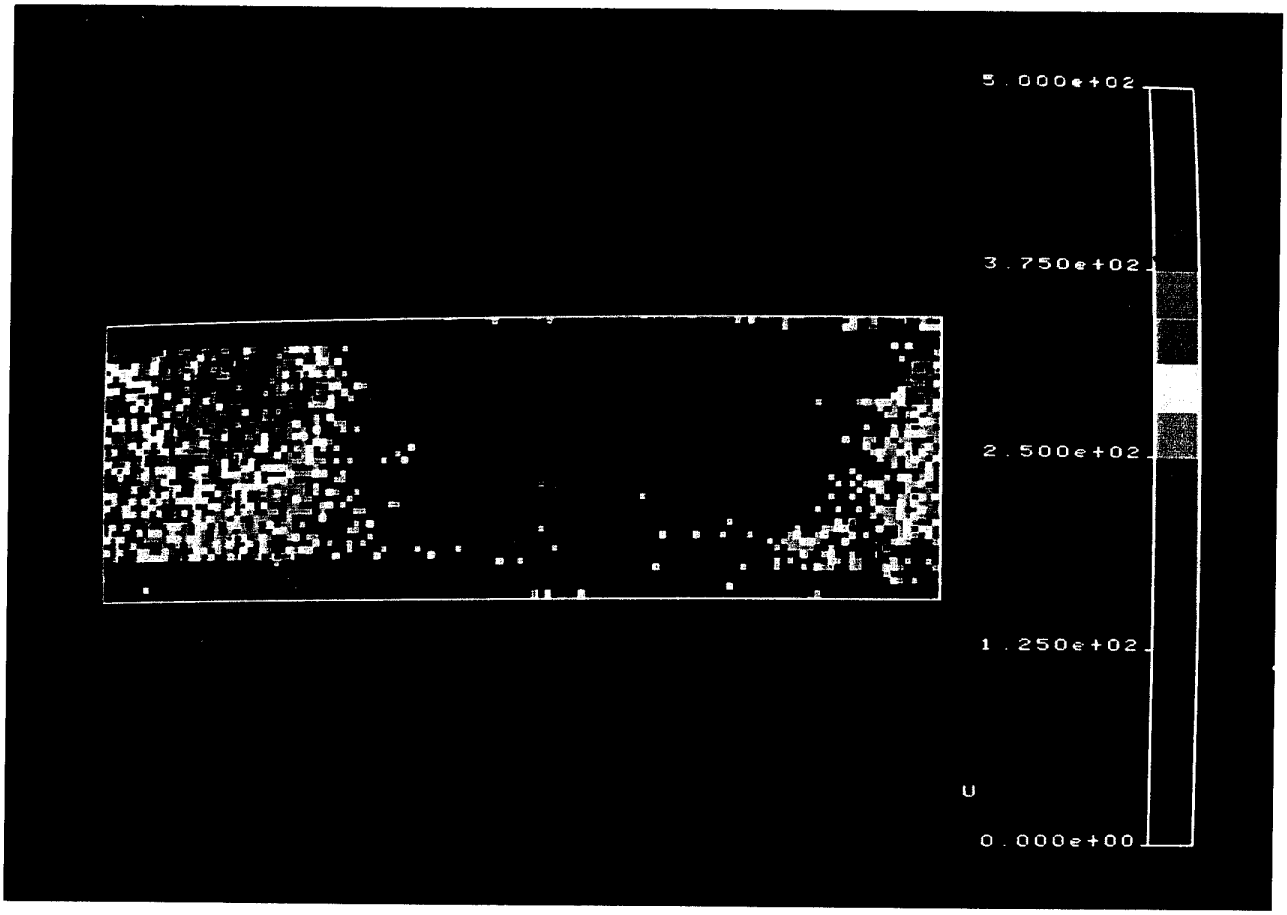

Figure 8: SPATE Region 3

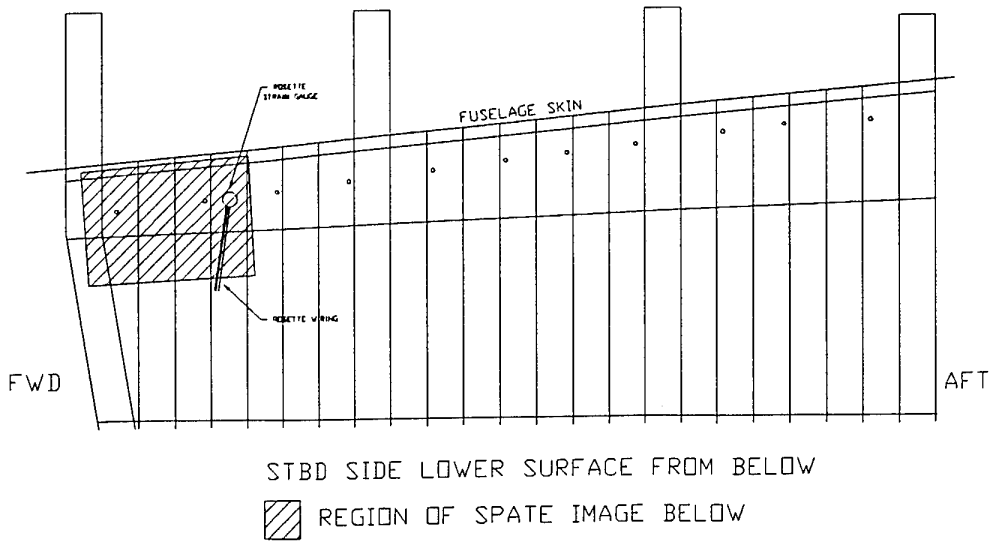

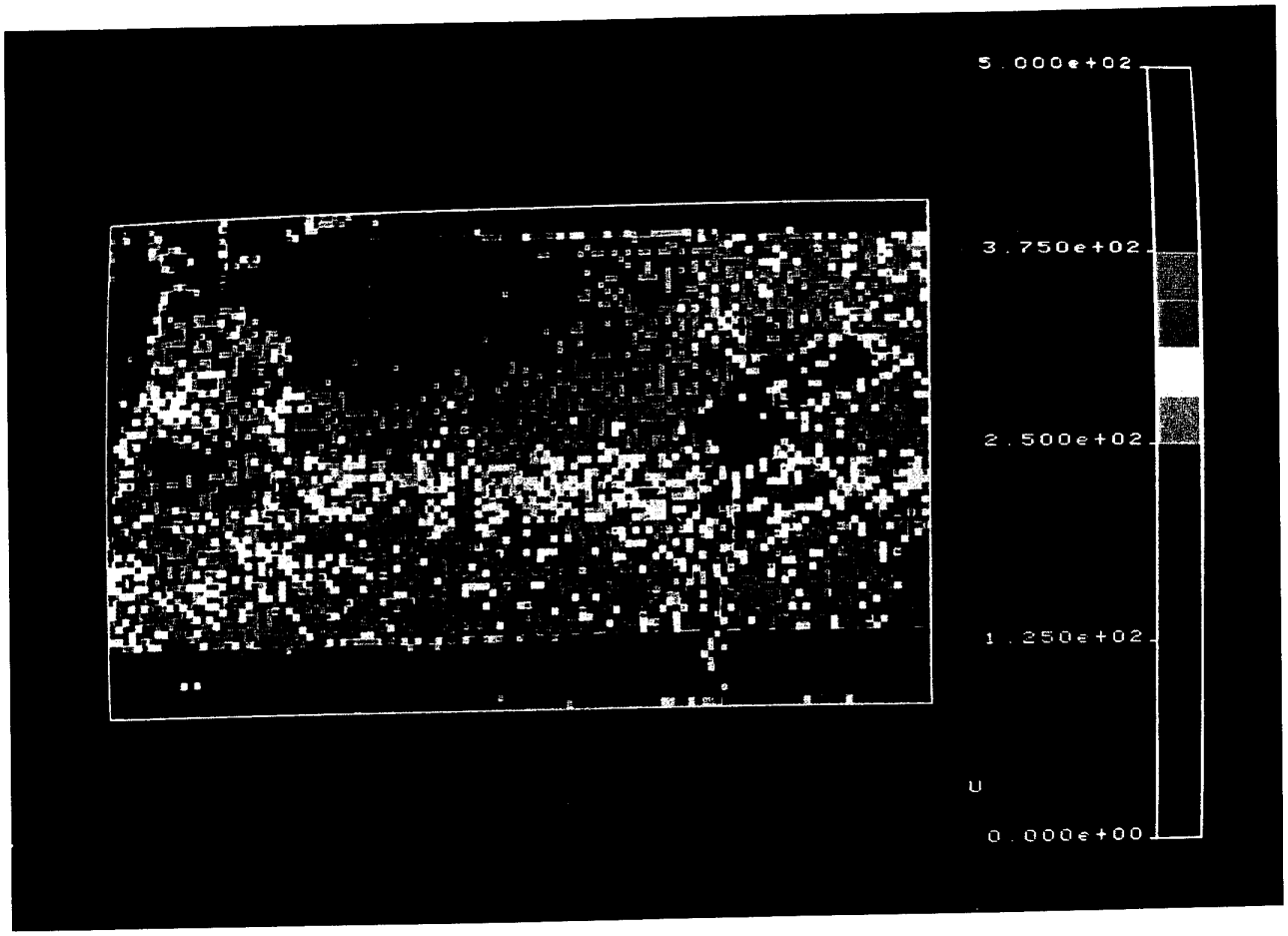

Figure 9: SPATE Region 4

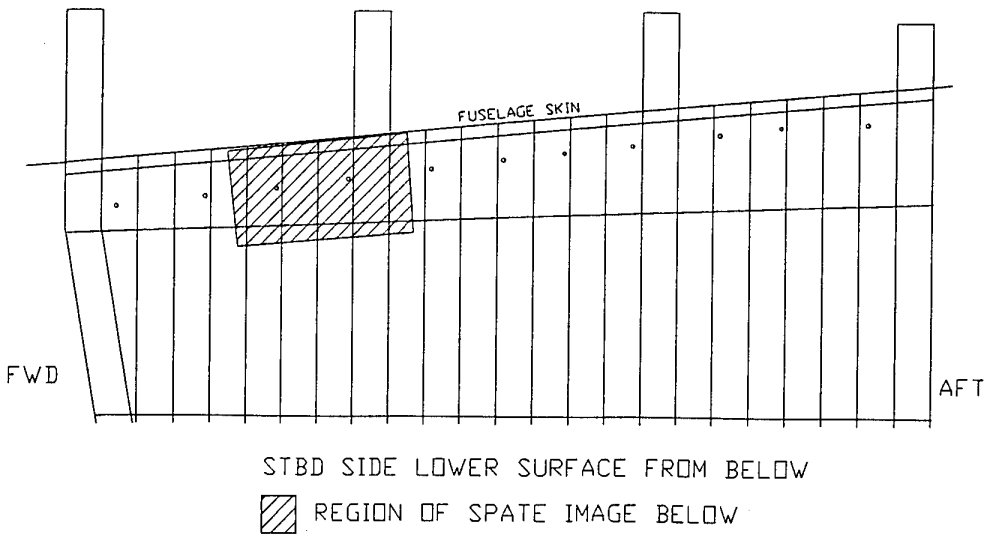

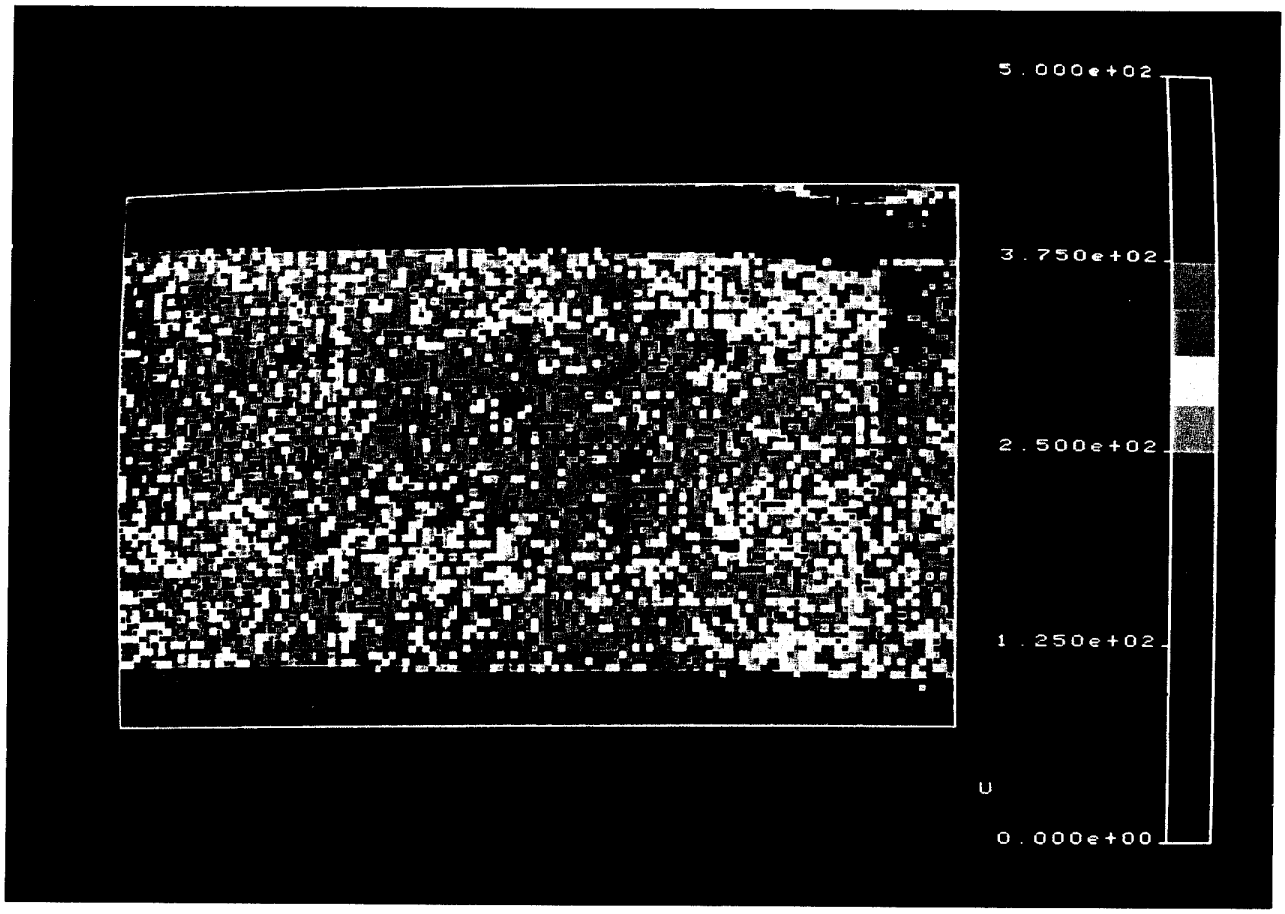

Figure 10: SPATE Region 5

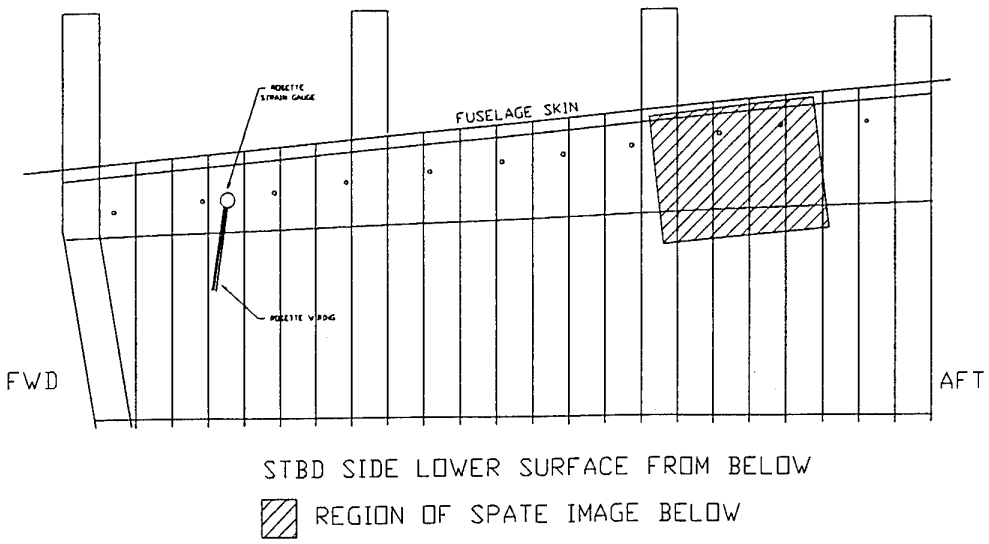

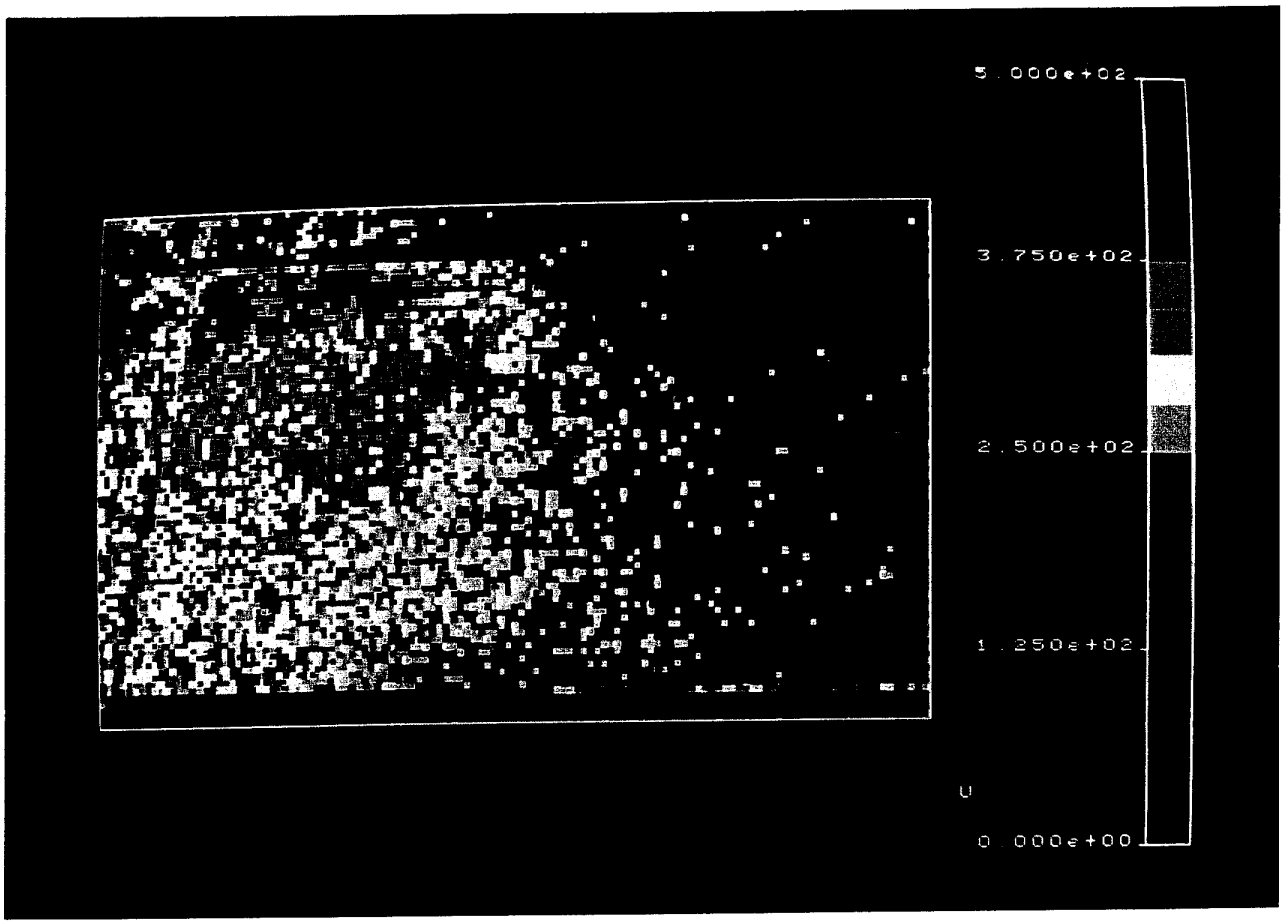

Figure 11: SPATE Region 6

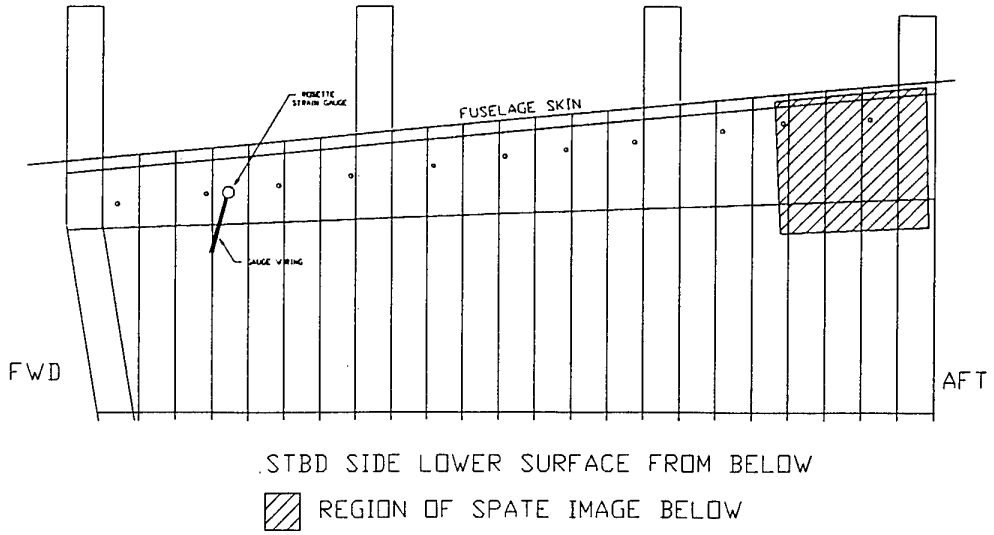

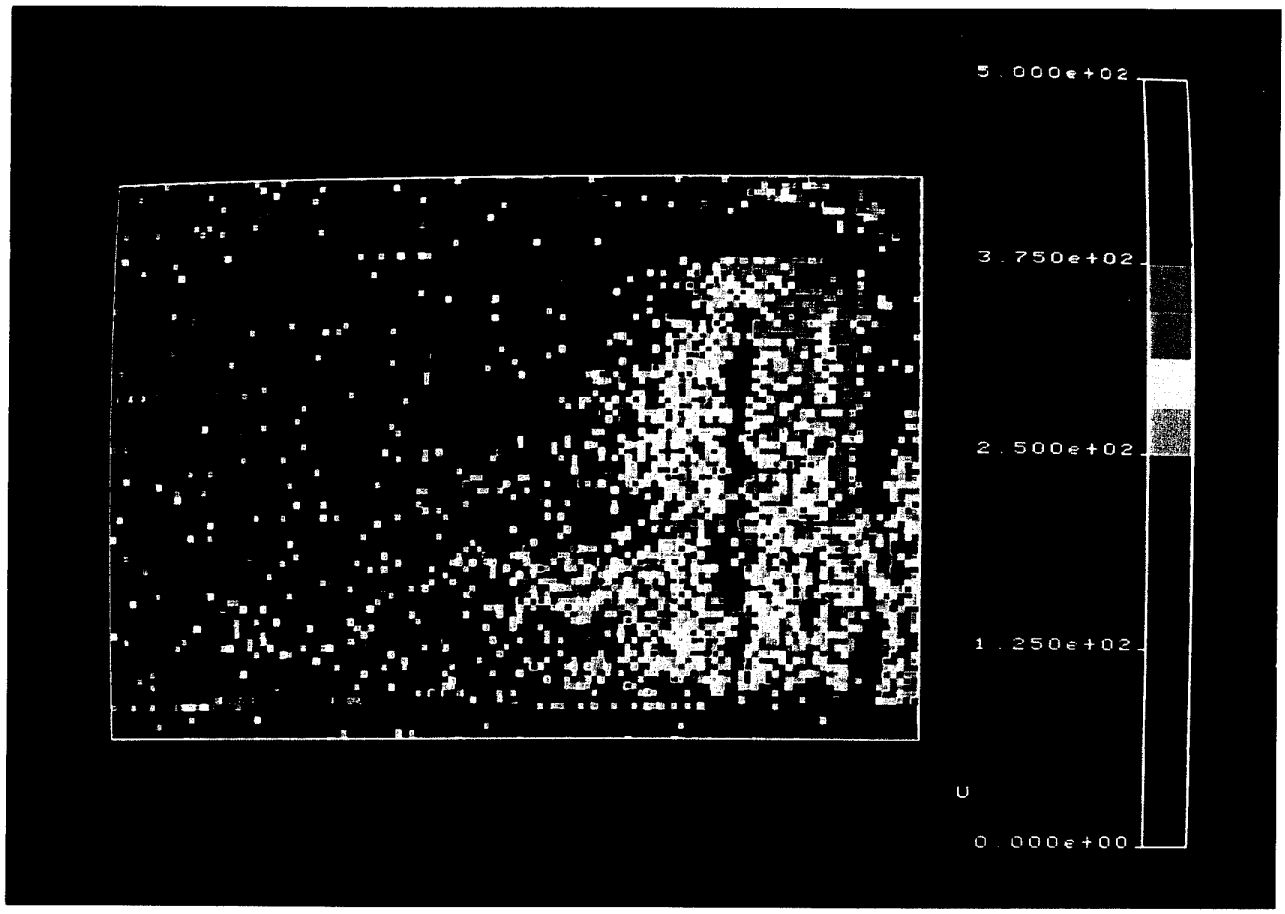

Figure 12: SPATE Region 7

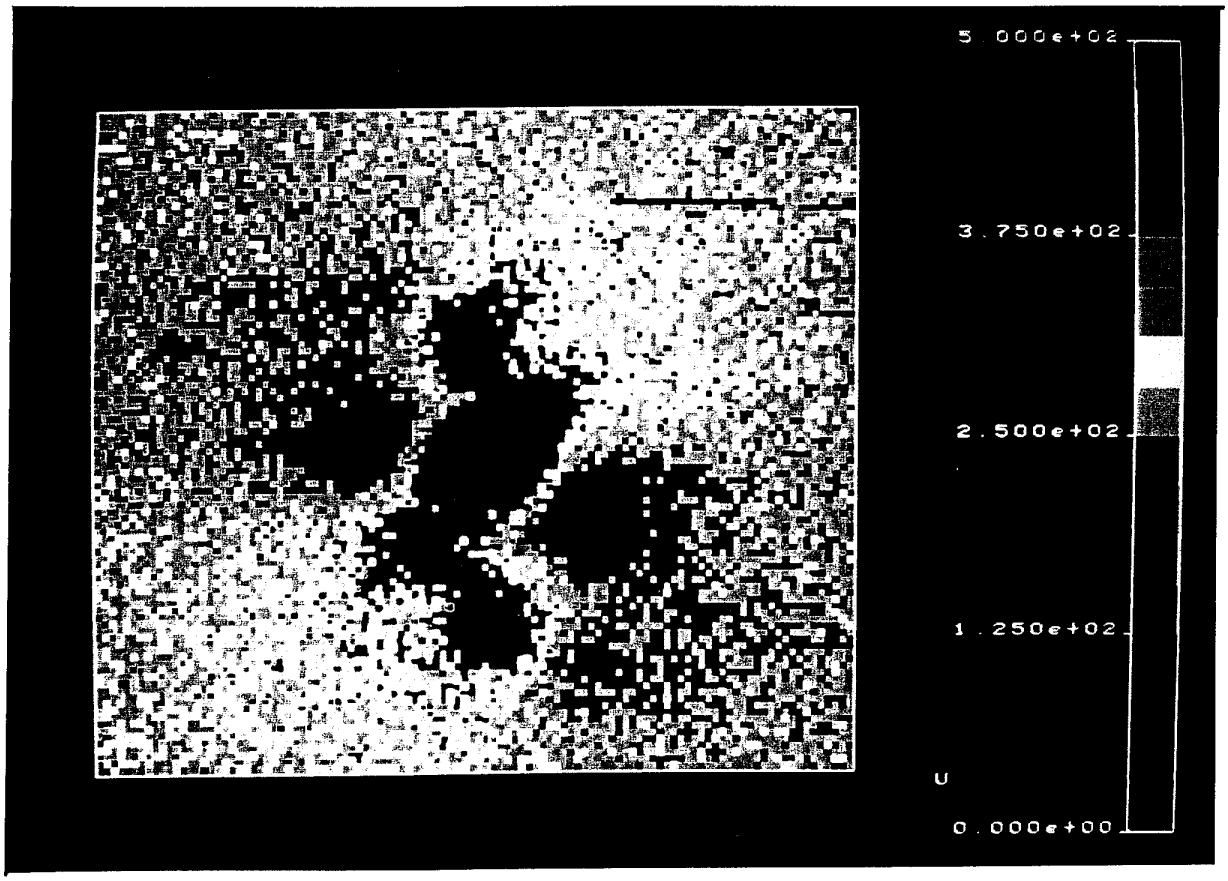

Figure 13: SPATE Scan of an Open Fastener Hole

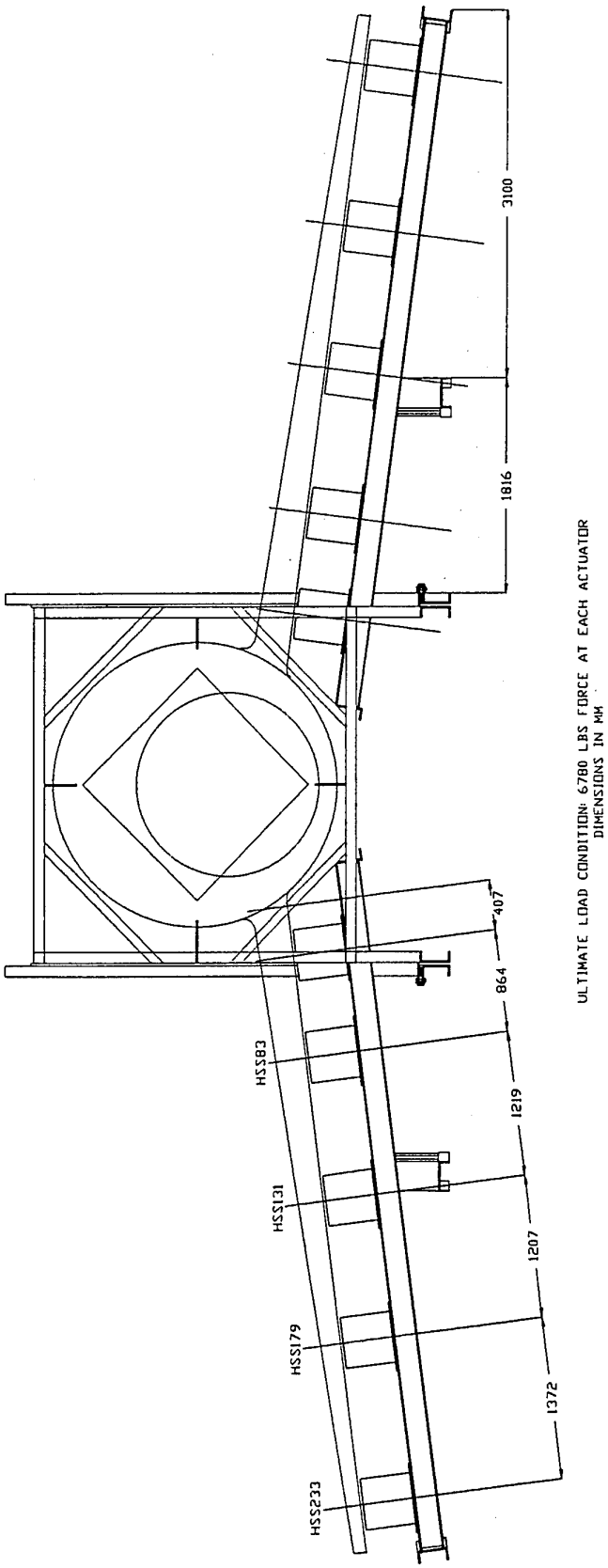

Figure 14: Loading Arrangement

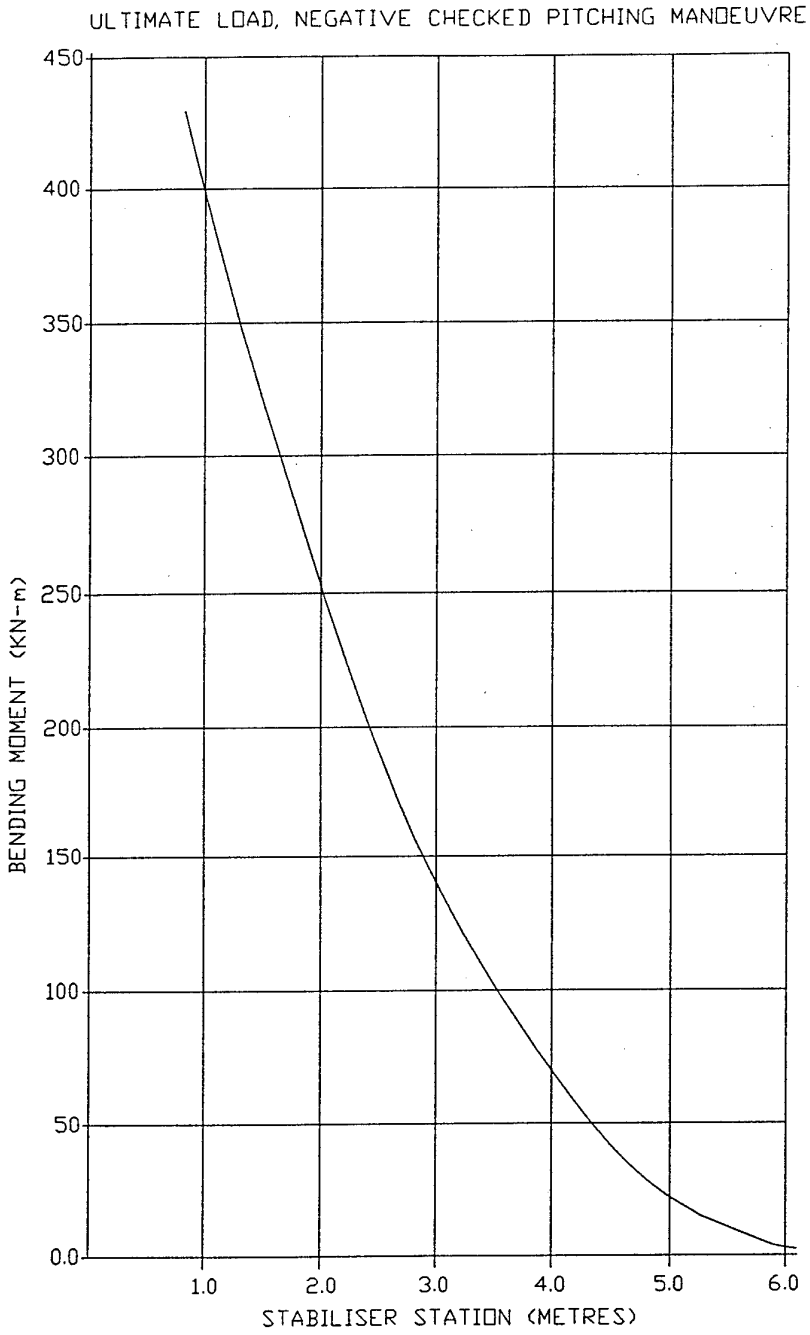

Figure 15: Ultimate Load Bending Moment Distribution

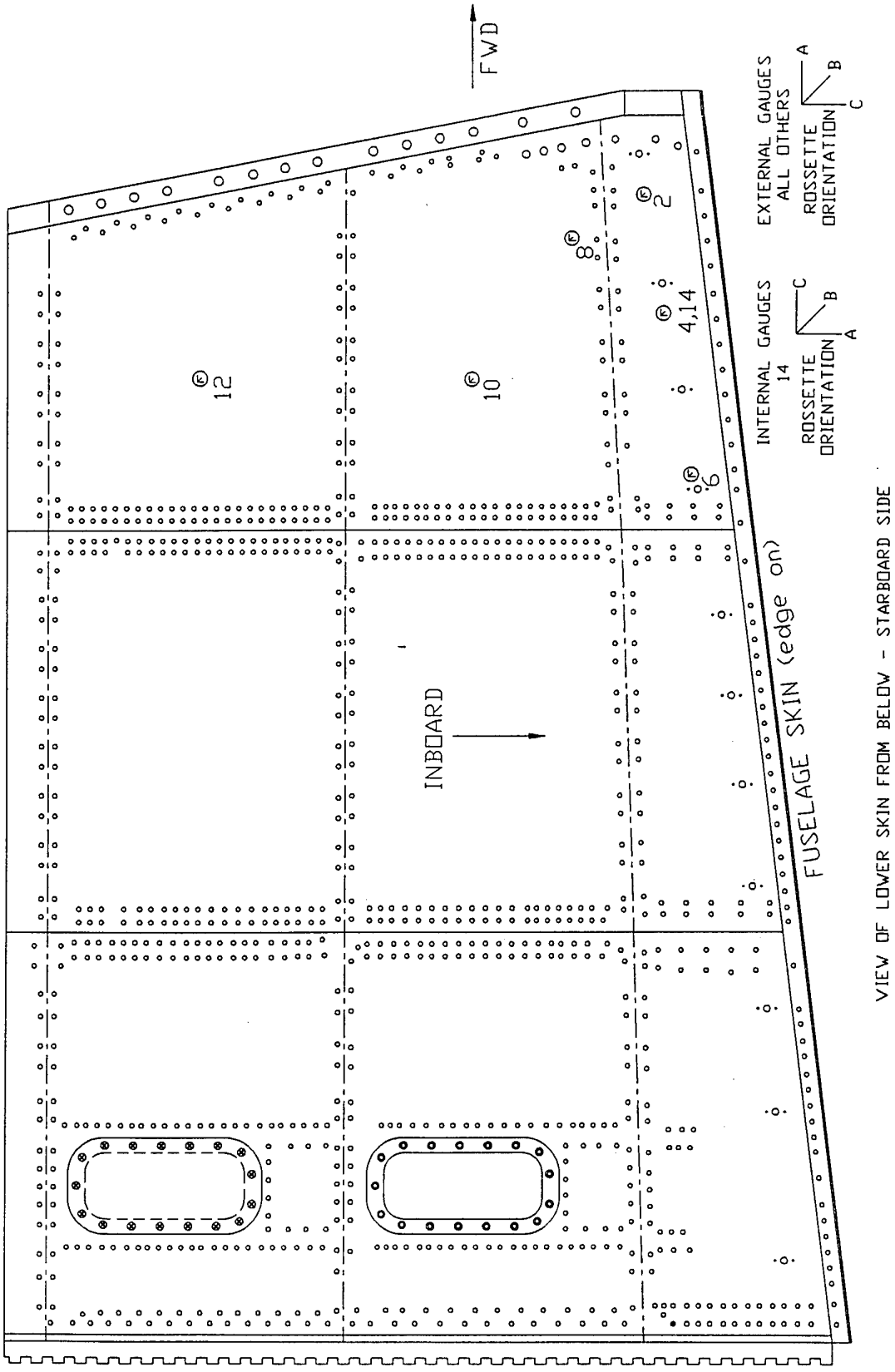

Figure 16: Strain Gauge Locations, Starboard Side

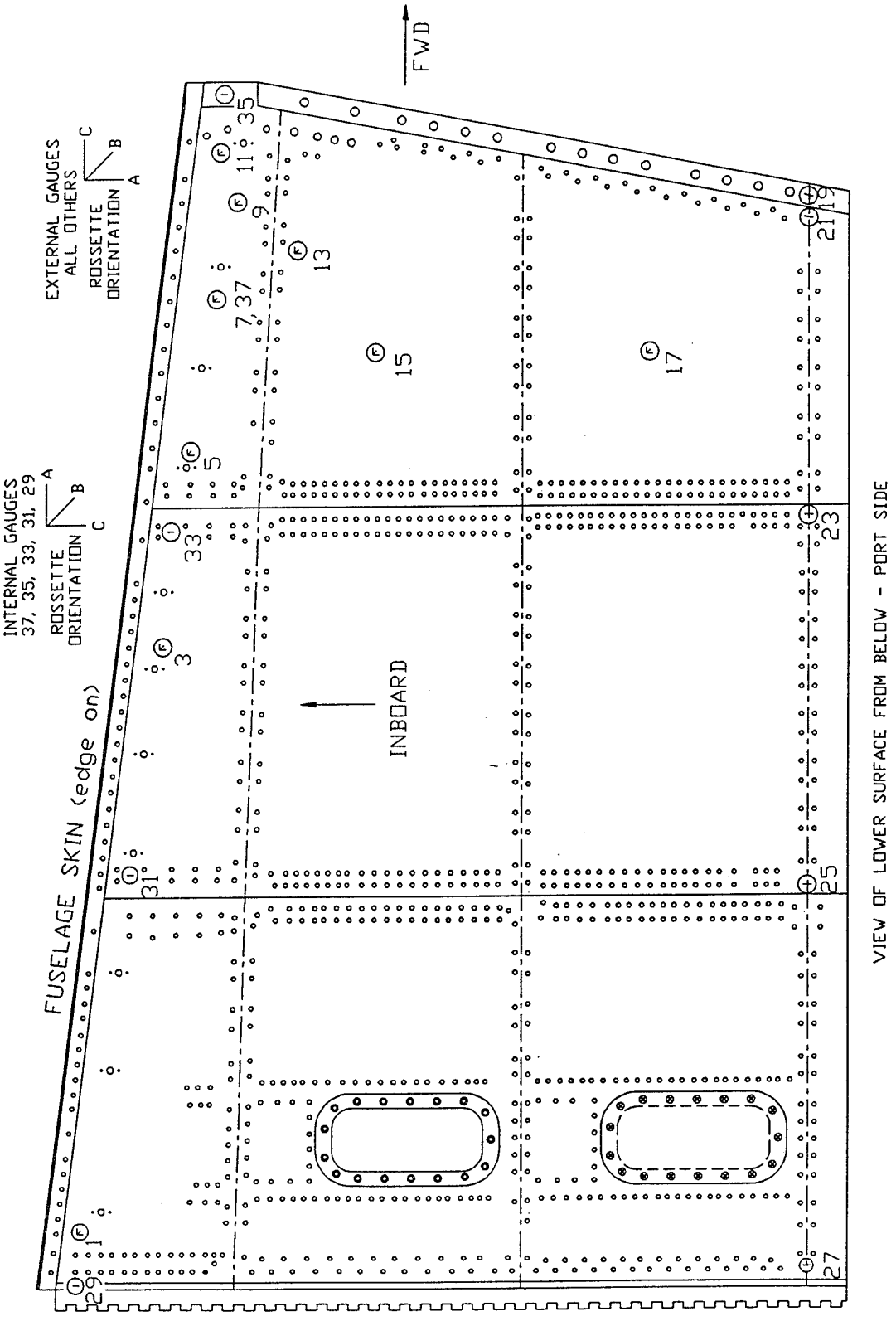

Figure 17: Strain Gauge Locations, Port Side

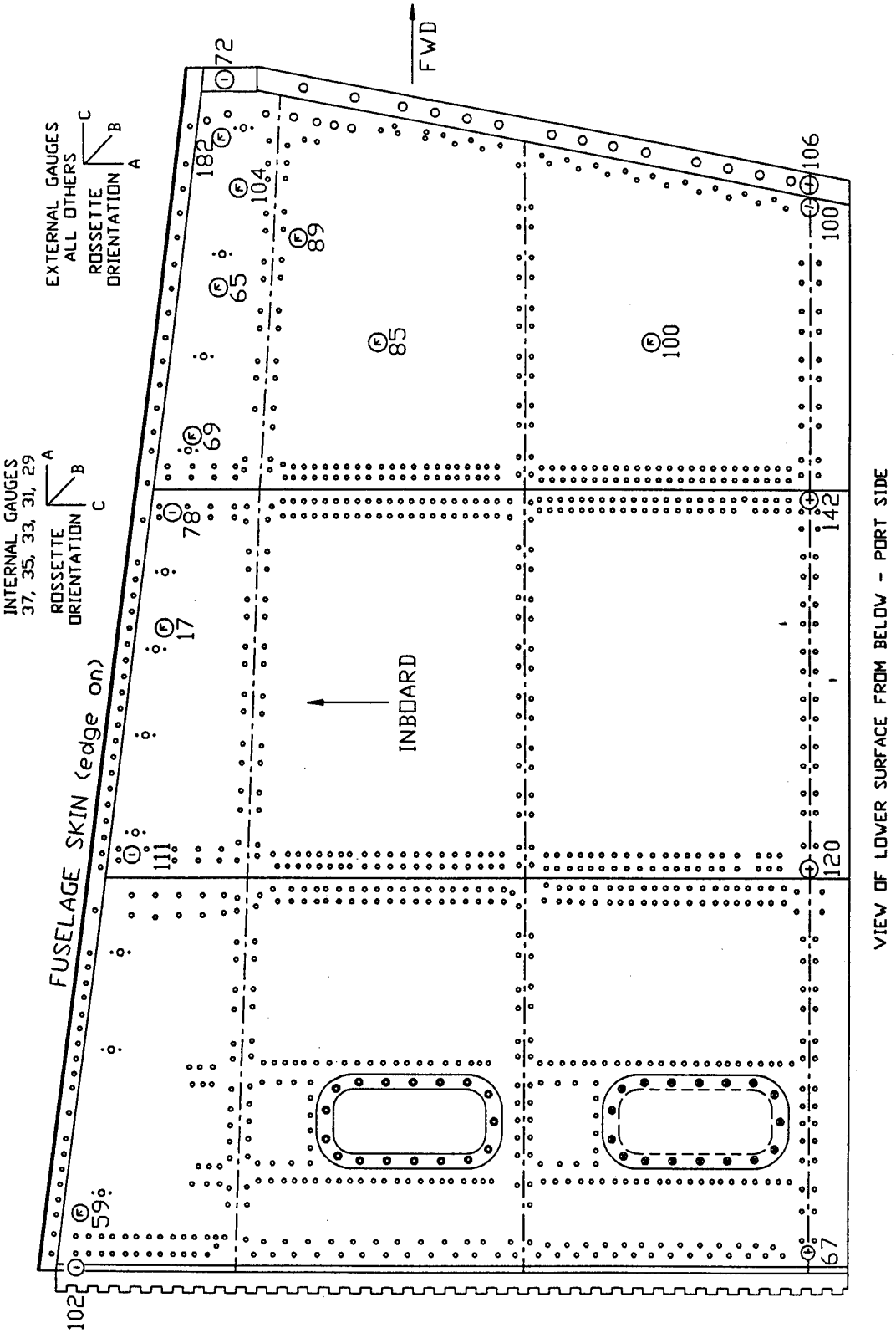

Figure 18: Spanwise Stresses (Compressive) at 60% of Limit Load in MPa

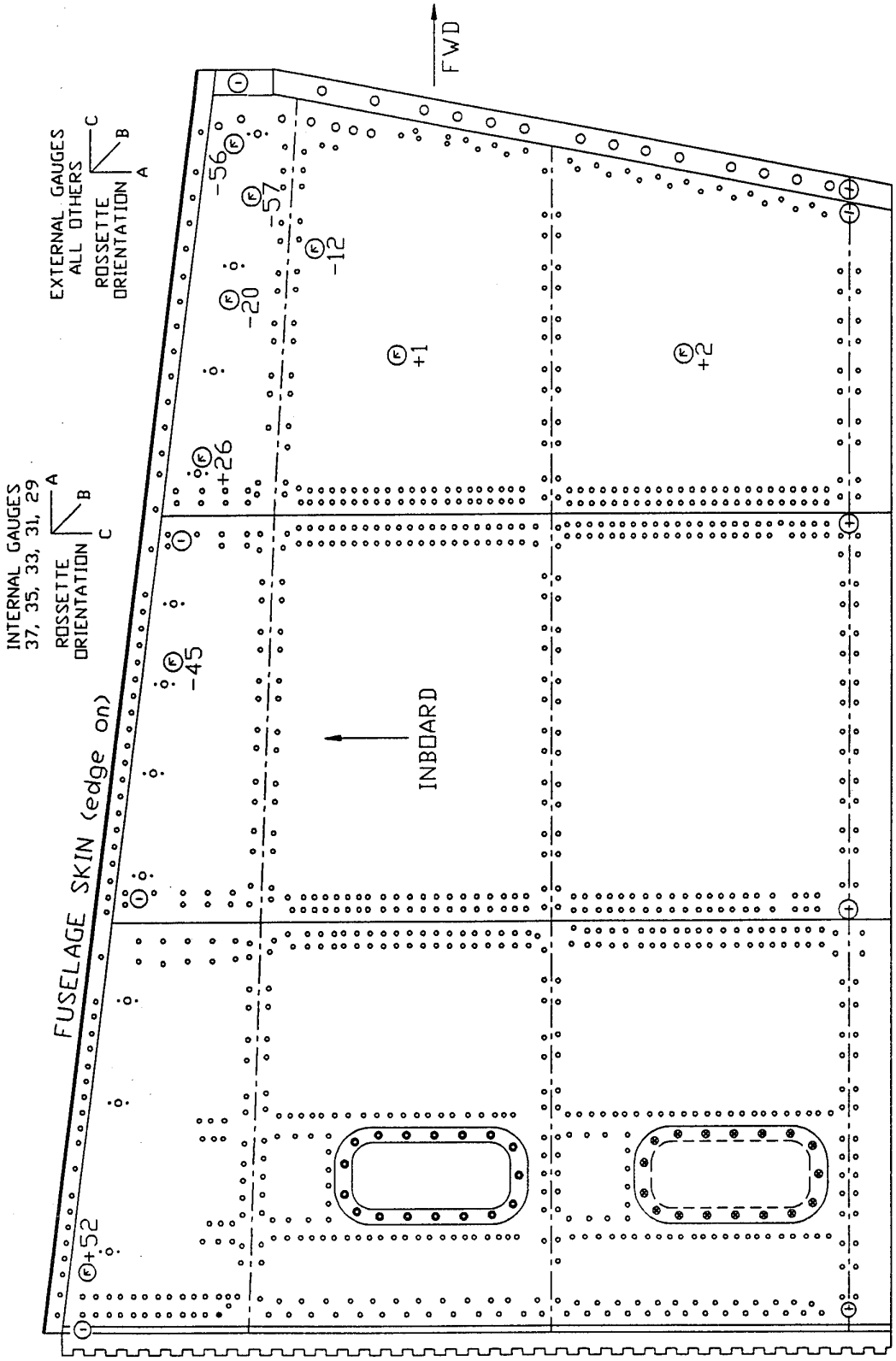

Figure 19: Shear Stresses at 60% of Limit Load in MPa

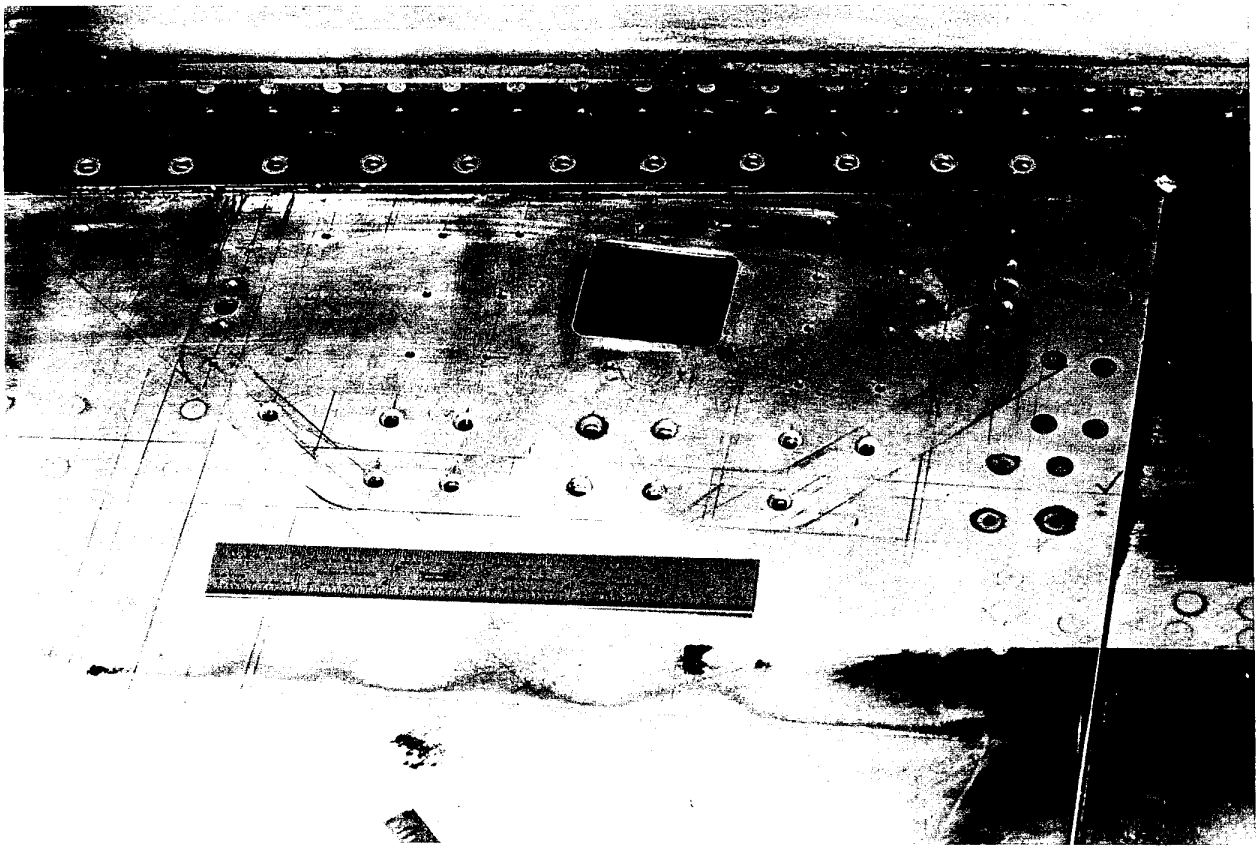

Figure 20: Standard Repair at Preliminary Stage

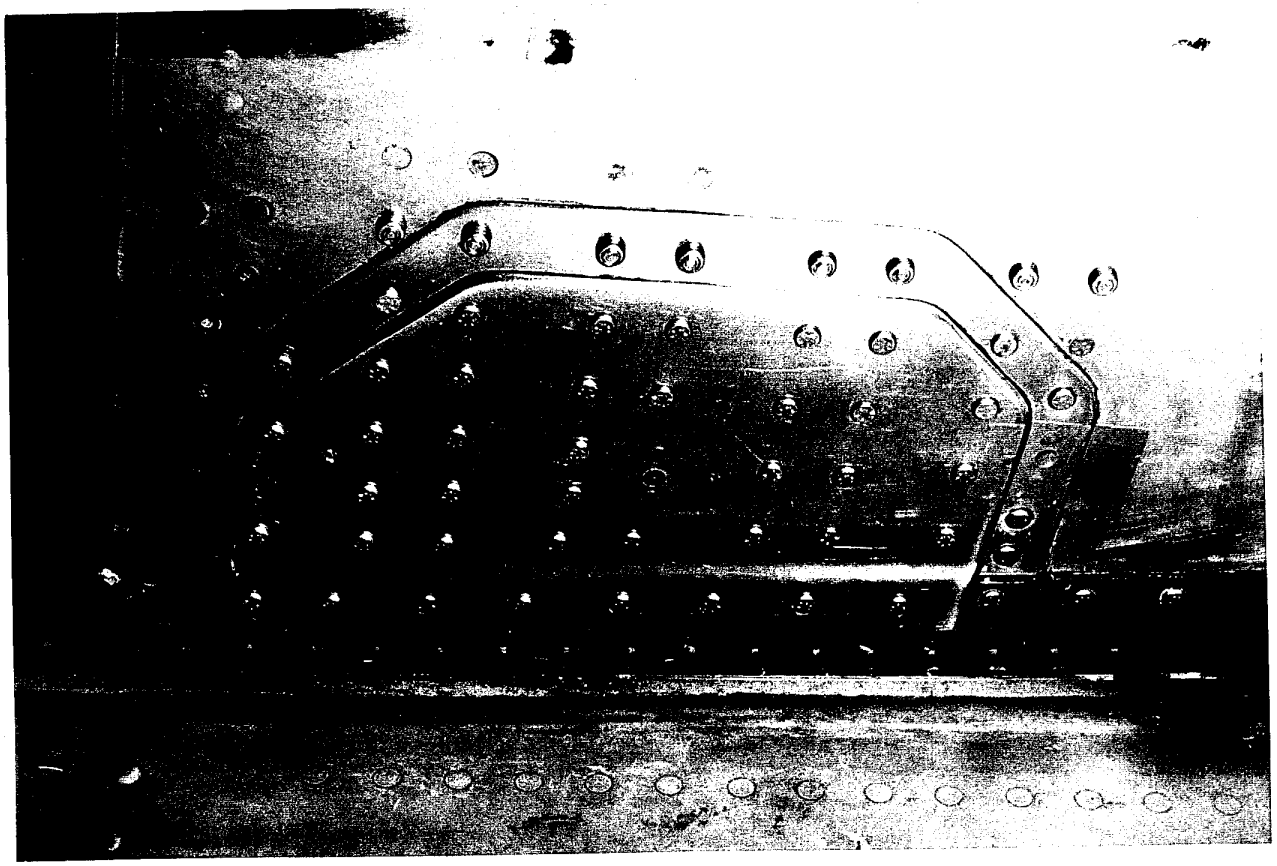

Figure 21: Standard Repair on Completion

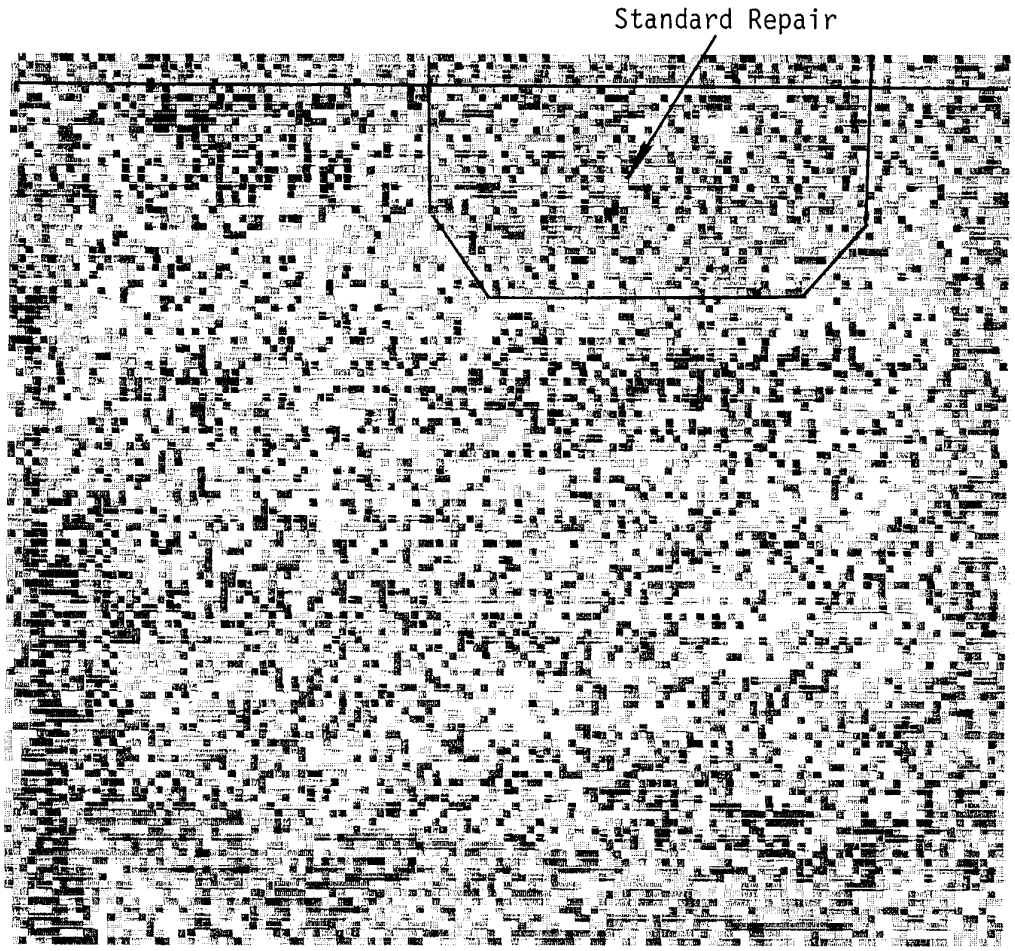

Figure 22: SPATE Image of Standard Repair

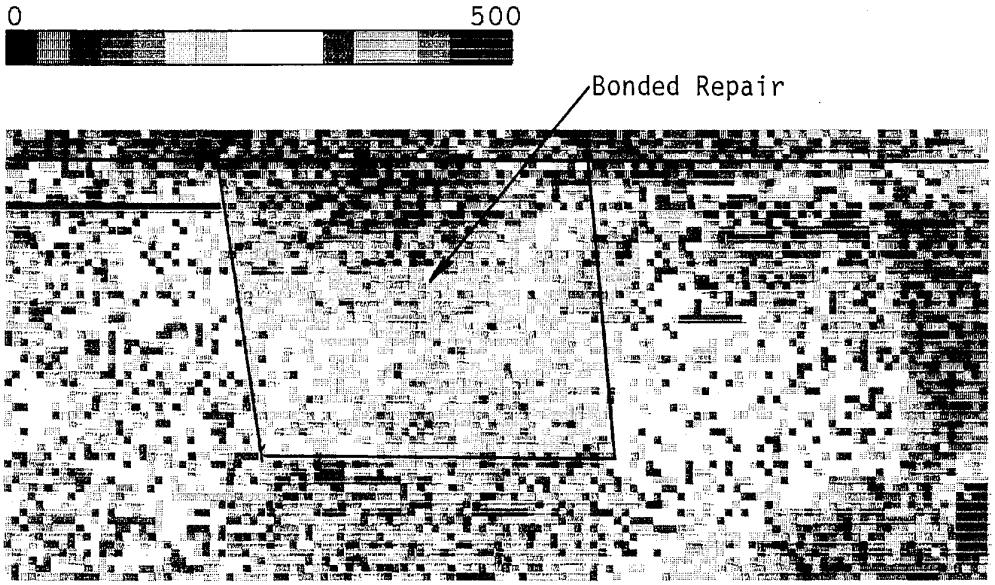

Figure 23: SPATE Image of Bonded Repair

DISTRIBUTION LIST

Orion P3C Horizontal Stabiliser Strain Survey and Corrosion Repair Development

R.H. Kaye, R. Jones and P. Hayes

(DSTO-TR-0196)

AUSTRALIA

DEFENCE ORGANISATION

Defence Science and Technology Organisation

Chief Defence Scientist
FAS Science Policy
AS Science Corporate Management
} shared copy

Counsellor Defence Science, London (Doc Data Sheet only)
Counsellor Defence Science, Washington (Doc Data Sheet only)
Scientific Adviser to Thailand MRD (Doc Data Sheet only)
Scientific Adviser to the DRC (Kuala Lumpur) (Doc Data Sheet only)
Senior Defence Scientific Adviser/ScientificAdviser Policy and Command (shared copy)
Navy Scientific Adviser
Scientific Adviser - Army (Doc Data Sheet and distribution list only)
* Air Force Scientific Adviser
Director Trials

Aeronautical and Maritime Research Laboratory

* Director AMRL
* Chief Airframes and Engines Division
* RLFM
* RLACS
* Kevin Walker
* Richard Callinan
* R. Kaye
* R. Jones
* P. Hayes
* D. Rowlands

DSTO Library

* Library Fishermens Bend
Library Maribyrnong
Main Library DSTOS (2 copies)
Library, MOD, Pyrmont (Doc Data sheet only)

Defence Central

OIC TRS, Defence Central Library
Officer in Charge, Document Exchange Centre (DEC), 11 copies
Defence Intelligence Organisation
Library, Defence Signals Directorate (Doc Data Sheet only)

DISTRIBUTION LIST
(Continued)

(DSTO-TR-0196)

Air Force

* OIC ATF ATS, RAAFSTT, WAGGA (2 copies)
* SQNLDR Peter Yates, ATS1, Logistics Systems Agency, Laverton
* SQNLDR Tony Dale, MPLM, RAAF Edinburg
* FLTSGT Tom Barton, RAAF Laverton
* Mr Max Davis, ATSIA, 501 Wing, RAAF Amberley
* Director General, Force Development (Air)
* Director of Air Warfare
* AWWSEW in DAW
* WGCDR Greg McDougall, CO 386 Squadron, RAAF Base, Richmond

HQADF

* DD-EW

RANTEWSS

* OIC

Army

Director General Force Development (Land), (Doc Data Sheet only)
ABCA Office, G-1-34, Russell Offices, Canberra (4 copies)

UNIVERSITIES AND COLLEGES

Australian Defence Force Academy
Library
Head of Aerospace and Mechanical Engineering
Deakin University, Serials Section (M list)), Deakin University Library, Geelong, 3217,
Senior Librarian, Hargrave Library, Monash University

OTHER ORGANISATIONS

NASA (Canberra)
AGPS

ABSTRACTING AND INFORMATION ORGANISATIONS
INSPEC: Acquisitions Section Institution of Electrical Engineers
Library, Chemical Abstracts Reference Service
Engineering Societies Library, US
American Society for Metals
Documents Librarian, The Center for Research Libraries, US

INFORMATION EXCHANGE AGREEMENT PARTNERS
Acquisitions Unit, Science Reference and Information Service, UK
Library - Exchange Desk, National Institute of Standards and Technology, US
National Aerospace Laboratory, Japan
National Aerospace Laboratory, Netherlands

SPARES (Normally 10 copies)

** Colour copies to be sent to addressees with asterisks*

DEFENCE SCIENCE AND TECHNOLOGY ORGANISATION DOCUMENT CONTROL DATA	1. PAGE CLASSIFICATION UNCLASSIFIED 2. PRIVACY MARKING/CAVEAT (OF DOCUMENT)

3. TITLE	4. SECURITY CLASSIFICATION (FOR UNCLASSIFIED REPORTS THAT ARE LIMITED RELEASE USE (L) NEXT TO DOCUMENT CLASSIFICATION)
Orion P3C horizontal stabiliser strain survey and corrosion repair development	Document (U) Title (U) Abstract (U)
5. AUTHOR(S) R.H. Kaye, R. Jones and P. Hayes	6. CORPORATE AUTHOR Aeronautical and Maritime Research Laboratory PO Box 4331 Melbourne Vic 3001

7a. DSTO NUMBER	7b. AR NUMBER	7c. TYPE OF REPORT	8. DOCUMENT DATE
DSTO-TR-0196	AR-009-445	Technical Report	November 1995

9. FILE NUMBER	10. TASK NUMBER	11. TASK SPONSOR	12. NO. OF PAGES	13. NO. OF REFERENCES
M1/9/96	AIR 94/118	ATS1, LSA	40	13

14. DOWNGRADING/DELIMITING INSTRUCTIONS	15. RELEASE AUTHORITY
To be reviewed three years after date of publication	Chief, Airframes and Engines Division

16. SECONDARY RELEASE STATEMENT OF THIS DOCUMENT

Approved for public release

OVERSEAS ENQUIRIES OUTSIDE STATED LIMITATIONS SHOULD BE REFERRED THROUGH DOCUMENT EXCHANGE CENTRE, DIS NETWORK OFFICE, DEPT OF DEFENCE, CAMPBELL PARK OFFICES, CANBERRA ACT 2600

17. DELIBERATE ANNOUNCEMENT

Announcement of this report is unlimited

18. CASUAL ANNOUNCEMENT YES/NO (Cross out whichever is not applicable)

19. DEFTEST DESCRIPTORS

Stress corrosion, Stress corrosion cracking; Bond stress; Stress concentration; Corrosion prevention; Stress distribution; Skin friction; Strain gages

20. ABSTRACT

This report presents results of an experimental investigation into the stress/strain field at the lower skin root region of the P3 horizontal stabiliser. Thermo elastic and strain gauge methods were used with a bare structure P3 tail-plane loaded under laboratory conditions. Applied load was restricted to 60% of design limit by the nature of the test article and the loading rig. The results show that the stresses in the region of interest are predominantly spanwise in direction. Stress concentrations consisting typically of 30% in-plane shear stress and 70% spanwise stress were found to occur near the inboard corners of each of the three lower skin planks. The largest of these was found at the forward corner of the forward plank. The load transfer between the skin panels and the spars was found to take place over the inboard 100mm of the stabiliser.

A bonded repair to corrosion damage has been presented on the basis of the bonded joints in the repair being stronger than the surrounding parent material. This repair design is not in any way dependent on the stress/strain test results and falls within the requirements of the recently produced RAAF Engineering Standard C5033. The region has a complex stress distribution due to the stabiliser skin panels terminating at the fuselage. Laboratory investigation of this stress distribution has been brought about by the availability of a suitable test article and has provided valuable ancillary information.